L13 P3

$O_3 + O_2 \sim fig\ 10$

SOME ASPECTS OF SOIL MECHANICS MODEL TESTING

by

R. G. James *

CUED/C - SOILS/TR 1971 No.6

* Assistant Director of Research
Department of Engineering,
University of Cambridge.

INTRODUCTION

Due to the complex mechanical behaviour of real soil there are considerable difficulties in obtaining accurate solutions to the boundary value problems of soil mechanics. The majority of present day methods of solution depend upon mathematical idealisations of the soil stress strain behaviour to either perfectly plastic or perfectly elastic. For the majority of problems both of these idealisations are unrealistic, and as a consequence the predictions made by conventional methods of analysis are prone to error. In addition to the difficulties of idealising the mechanical behaviour of the soil, the problems themselves are usually of a complex nature, e.g. the problem of a pier foundation rotating about its upper surface as portrayed in Fig.1 and discussed by Roscoe (1970) in the Tenth Rankine Lecture.

Consequently experimental investigation of the load displacement relationships for the boundary value problems of soil mechanics is essential. Testing of full scale prototype structures, although very necessary, is expensive and time consuming, and therefore the incentive and need to perform representative model tests is great. One may broadly classify model testing, dependent upon the prime objectives, into three distinct, but interrelated, categories. These categories will be referred to as Category I, II and III.

CLASSIFICATION OF MODEL TESTING

Category I model tests are defined as being concerned only with predicting the behaviour of a specific prototype structure from that of the model. Any special ground conditions, i.e. soil strata, water conditions etc., such as illustrated in Fig.2a for a pad foundation problem, must be suitably simulated in the model,

and so the results obtained do not have general applicability. In this type of model test the principles of similarity must be satisfied before the results can be of practical use (e.g. Sutherland (1965)). However, the general principles discussed by Rocha (1957) and Roscoe (1968) should ensure wider application of this type of model test, especially in the area of centrifugal model testing which allows the use of 'prototype' soil at prototype stress levels and under approximately correct conditions of stress and strain paths. Possibly one of the major advantages of centrifugal model testing is that processes such as primary consolidation occur very much faster in the model than in the prototype, i.e. time is modelled as N^2 where N is the model scale. Thus for a $\frac{1}{60}$ scale model $2\frac{1}{3}$ hours in the model is equivalent to 1 year in the prototype.

The second approach to modelling, defined as Category II, is to consider that the model is a small prototype structure itself and to compare its behaviour with that predicted by some method of analysis. For this approach to be useful it is of utmost importance that the model conforms with the assumptions inherent in the method of analysis adopted. Typical requirements would be that the soil is in a uniform state and that the influence of the boundaries of the container of the model may be ignored, e.g. as illustrated in Fig.2b for the bearing capacity problem. From the results of such tests it should be possible to assess the accuracy of various methods of analysis and also to confirm that the soil constants established from fundamental testing apparatus relevant to the stress conditions in the model can be used to predict the performance of the model. The results obtained

from such tests are not necessarily of immediate use in the design of a complex full scale prototype, but are of great value in establishing certain design principles. Experiments of the above two types are inherently restricted by the need to simulate real problems. This automatically leads to a third type of model test, defined as Category III, of which the full scale need never exist, but which is designed specifically to reveal detailed stress and deformation information about a problem. The prime objectives of this type of test are to increase the understanding of the soil behaviour, and the soil structure interaction, such that new methods of analysis may be developed which in turn will lead to better design rules for use in the future. Such a model experiment, a narrow wall rotating about its toe into sand, is illustrated in Fig.2c. By employing such a 'thin' plane strain model it is possible by radiography to obtain detailed information on the soil strain behaviour not possible on wider plane strain or 'three dimensional' models.

L 13 P3

In the past numerous workers have performed a variety of experiments falling into the above mentioned categories. It is not possible to mention all here, but a few examples will be given to illustrate the categories further. Good examples of Category I type tests are to be found in the field rather than the laboratory and exist in the form of instrumented trial earth structures, ie. test embankments. In certain cases nature has already carried out full scale tests in the form of natural slope failures, and in cases where careful site investigation establishes the relevant soil parameters and ground water conditions these tests produce valuable comparisons between theory and "experiment", (e.g. Skempton and Hutchinson (1969)).

Without a centrifuge it is in general extremely difficult to perform representative small scale Category I type tests, due to the difficulty of modelling the soil. With the centrifuge, however, this major difficulty may be overcome, since providing the soil grain sizes are sufficiently small the prototype soils may be used in the model. Examples of such tests are given by Schofield and Lyndon (1970) on the short term stability of slopes in overconsolidated clay, and by Endicott (1971) on the settlements of a granular fill embankment sited on a substrata of soft clay and peat. Fig.3 shows the soil strata beneath the embankment and Fig.4 the displacements corresponding to 'end of construction' and at a time corresponding to 1.3 years later. In the main the above mentioned tests were designed specifically to simulate real prototype behaviour and thus may be considered to fulfil the requirements of Category I tests.

There are numerous examples of Category II type tests, since in general the majority of soil mechanics model testing falls into this category. One good example in Europe is the 'large' scale footing tests performed at Karlsruhe University reported by Leussink, Blinde and Abel. They tested instrum ented foundations up to 1.5 metres square, in a 9 x 9 x 3 metre pit filled with uniformly compacted sand (see Fig.5). Due to the large size of their model they were able to determine the normal pressure distribution beneath their footing in great detail.

The work on passive walls reported by Rowe and Peaker (1965) represents a classic example of Category II type tests. They translated a vertical wall at various angles to the horizontal into sand, observing the mobilised angle of wall friction (δ), the normal pressure distribution, load displacement relationships and

modes of failure. Typical results for two directions of wall movement into dense sand are reproduced in Figs.6(a) and (b). Some of the stress strain properties of the sand employed are also shown in Fig.6(c). Study of these figures reveals three important features: (i) the importance of the direction of wall movement, i.e. the wall which was translated upwards at 45^0 to the horizontal has a peak passive earth pressure coefficient K_p of only 3.0 whereas the wall translated approximately horizontally generated a peak K_p of approximately 7.4.

(ii) the quite different load displacement relationships for the two directions of movement, and

(iii) the peak value of mobilised ϕ obtained by back analysis employing conventional theory is considerably less than the peak ϕ observed in the plane strain tests, i.e. ϕ_m observed in wall experiments of between 35^0 and 37^0 whereas peak ϕ measured in fundamental plane strain test is approximately 43^0.

Rowe and Peaker explain this latter feature qualitatively by postulating the mechanism of progressive failure. I have mentioned Rowe and Peaker's observations in some detail, since clearly in order to describe quantitatively the mechanism of progressive failure appropriate Category III experiments need to be performed.

Examples of Category III type experiments, with cohesionless soils, are shown in the work of Brinch Hansen (1953) who observed rupture modes for a wide variety of idealised wall problems, and more recently in the work of Butterfield, Harkness and Andrawes (1970) who have observed the detailed displacement fields associated with the problem of the penetration of a sand mass by a rigid wedge.

Soil mechanics has now reached a stage in its development where the fundamental stress strain laws of engineering soils are beginning to be understood. At the same time engineers are under pressure to produce more economic designs and better predictions of soil structure performance. A prediction of whether a structure will stand up or fall down, although vital, is no longer adequate. There is therefore great need for experiments of the Category III type which should prove of great assistance in the development of more sophisticated methods of analysis which may then be brought into general use via Category II and I experiments.

SOME TYPICAL RESULTS OF A CATEGORY III EXPERIMENT AT CAMBRIDGE

I believe that the majority of the model work performed at Cambridge in the past decade under the leadership of Professor Roscoe would be classed as Category III. Roscoe's objectives were always to develop new and better theories via new experimental observations. Possibly the most important aspect of Category III model experiments of today is the detailed observation of strain phenomena. In order that such observations may be achieved it is necessary to work with relatively thin (6" - 9" thick) plane strain models employing test tanks with 'transparent' sides. Such models allow the detailed observation of soil displacements by photography or radiography, however only at the expense of introducing side friction effects. These effects may be minimised by suitable choice of materials and lubricants, but they may never be completely removed. A typical test facility is shown in Fig.7

which is a photograph of a model wall apparatus. The wall is 13" high and the test tank dimensions 96" x 60" x 7½". With this apparatus it is possible, with various modes of wall movement, to observe wall pressure distributions (both normal and shear) and the detailed soil displacement and strain behaviour. Typical strain results for the case of wall rotation about the top into dense Leighton Buzzard sand are shown in Fig.8 for three stages of rotation, i.e. θ = 0.5, 0.95 and 1.4^0 corresponding to 58, 83 and 97% of the peak load measured on the wall. The full line contours represent values of maximum shear strain and the broken lines trajectories of principal compressive strain. Considering Fig.8c it is quite clear that there is a large concentration of strain at the toe of the wall and that a substantial transition zone of deformation originates from this point. Fig.9 shows the corresponding observed trajectories of zero extension, i.e. 'slip lines' indicating a well defined zone of 'plastic' deformation. It is clear from these figures that the mode of failure, termed progressive, occurs in this experiment. Figs.10 and 11 show similar data for loose sand.

Typical stress ratio strain laws obtained from the simple shear apparatus for dense and loose Leighton Buzzard sand are shown in Fig.12. Using these relationships in conjunction with the strain data shown in Figs.8 and 10 it would be possible to define the mobilised shear strength throughout the deforming zones at any stage of deformation. Restricting such an exercise to the centre line of the transition zone, i.e. to a line passing through the peaks of the shear strain contours, it is possible to deduce the mobilised shear strength along the centre slip line. This exercise has been carried out for the data on dense sand presented in Fig.8 and the results are presented in Fig.13. In

this figure the mobilised stress ratio $\frac{t}{s}$ ($= \sin\phi_{mob}$) is plotted against the non-dimensional distance along the centre slip line $\frac{S}{H}$. The major point of interest in this figure is the curve OPQ corresponding to $\theta = 1.4^0$, i.e. at approximately peak load on the wall. Only the sand at point P has the fully mobilised peak stress ratio. The sand to the right of P, i.e. curve PQ has yet to mobilise its peak stress ratio, whereas the sand to the left of P, i.e. curve OP, has passed beyond its peak strength and is approaching the critical state strength. These curves indicate the danger inherent in constant ϕ analyses and the dubious nature of ever assuming a fully mobilised ϕ in soils problems.

In order to throw more light on the strain behaviour in this problem it is useful to replot the data shown in Figs.8 and 10 as the reciprocal of shear strain, i.e. $\frac{1}{\gamma_M}$ against the non-dimensional distance along the centre line of the transition zone $\frac{S}{H}$ for each stage of rotation. The results are shown in Figs.14 and 15 for dense and loose sand respectively. These figures are surprising in view of the apparently complex strain behaviour occurring in this problem. It would appear that the strain behaviour is adequately described at each stage of wall rotation by simple linear relationships. By plotting the wall rotation θ divided by the shear strain, i.e. $\frac{\theta}{\gamma_M}$ against $\frac{S}{H}$ it is possible to obtain single approximately unique relationships which are shown in Figs.16 and 17 for dense and loose sand respectively.

If one could apply a simple kinematic theory to the problem under consideration and could predict relationships similar to those observed, then in conjunction with an appropriate stress ratio strain law one would also be able to estimate the load-wall displacement relationships. With this aim in mind a simplified

approach to predicting the load-displacement relationship for this problem will be made in the next section. However, the observed strain distribution laws of Figs.16 and 17 will be employed rather than possible predictions.

A 'KINEMATIC' APPROACH TO THE SOLUTION OF A PASSIVE EARTH PRESSURE PROBLEM

James and Bransby (1971) postulated a slip line field for a constant dilatation rate material which with suitable boundary conditions allows predictions of strain distributions throughout deforming regions of a sand mass. The essential feature of the slip line field was that the bounding slip line, i.e. the slip line beyond which there was no movement, was a log spiral originating at the toe of the wall with its centre at the top of the wall, as illustrated in Fig.18. The equation of the spiral is $r = r_o e^{\psi \tan\nu}$ where r is the radius from the top of the wall to a point on the spiral, ψ the angle of this radius to the vertical, and ν the angle of dilatation, i.e. $\nu = \sin^{-1} \frac{\dot{v}}{\dot{\gamma}_M}$ where $\dot{v}$ and $\dot{\gamma}_M$ are the instantaneous volumetric and shear strain rates respectively. The spiral portion continues as far as $\psi = 45 + \frac{\nu}{2}$ and the upper portion of the bounding slip line is assumed to continue as a straight line inclined at $45 - \frac{\nu}{2}$ to the horizontal surface.

It will now be assumed that such a spiral and straight line defines the centre slip line of the transition zone, i.e. the slip line along which the experimental data indicate that the shear strains are a maximum for the problem of passive rotation of a wall about its upper edge. This assumption may be considered reasonable since for the given mode of wall movement such a slip

line represents the possible location of a 'kinematically admissible'* strong displacement discontinuity, and hence also the location of the largest strains. Since the strains are large, significant mobilised shear strengths are also implied and hence, in order that stress equilibrium be maintained, the material either side of such a slip line must also suffer large strains in order to develop sufficient strength. Thus the slip line can be taken to represent the centre line of a substantial transition zone. The precise boundaries of the transition zone are not easily defined since they are dependent not only on the kinematics of the problem but also upon the stress-strain properties of the soil. However, it is clear that the strains in the transition zone must be such that stress equilibrium is maintained along any slip line within it. For simplicity it will be assumed that a fan of slip lines originates at the toe of the wall, with an included angle of $45 - \frac{\nu}{2}$, and that the fan be inclined symetrically with respect to the centre slip line. The outer slip lines of this fan are considered to be the bounding slip lines of the transition zone, i.e. as portrayed in Fig.19. Thus the upper bounding slip line is defined by a ν log spiral with centre O_2, the centre slip line of the transition zone by a ν log spiral with centre O_1 and the lower bounding slip line by a ν log spiral with centre O_3. The above method of defining the transition zone and the slip lines within it is somewhat arbitrary; however, for the problem under consideration it produces a zone of slip lines similar to those observed experimentally.

The soil within the transition zone may be arbitrarily divided into triangular elements as shown in Fig.20. If the angles of the resultant stress vectors on the three sides of each

---

* Both the log spiral and straight line portions of this slip line are individually kinematically admissible for a constant ν material, however for the combination to be so the material above the slip line must suffer some deformation.

triangular element are known, then by considering the force equilibrium of each element and commencing the calculations from the uppermost triangular element, i.e. element 1 labelled HDJ in Fig.20(a) it is possible to establish the magnitudes of the resultant forces acting on every portion of the slip lines TABCD and TEFGHJ. Subsequently the resultant forces acting on a particular slip line may be summed vectorily and by consideration of the force equilibrium of the 'block' of material above that slip line the magnitude and direction of the resultant force on the wall may be determined, i.e. as shown in Fig.20(b).

The advantages of such a method of calculation are (i) that both magnitude and direction of the resultant wall force are defined, whereas in most conventional methods the angle δ has to be assumed, and (ii) that different material properties may be assumed for each triangular element specified in the transition zone. In a conventional calculation method it is usually assumed that lines of slip are also planes of maximum stress obliquity, and thus the angles of the stress vectors along such a line are usually assumed to be at ϕ to the normals. In the present calculation since the slip lines are lines of zero extension the stress vector will be inclined at ζ to the normal as shown in Fig.20(b). The relationship between $\sin\phi$, the mobilised shearing resistance, ν, the dilatation rate (i.e. $\sin\nu = \frac{\dot{v}}{\dot{\gamma}_m}$) and ζ is given by equation 1.

$$\tan\zeta = \frac{\sin\phi_m \cos\nu}{1 - \sin\phi_m \sin\nu} \qquad \ldots\ldots\ldots \quad (1)$$

which is obtained directly from Mohr's circles of stress and strain rate by assuming that axes of stress and of strain rate are coincident.

Employing the empirical relationship $\gamma_M = 1.47 \frac{H\theta}{S}$ in the case of dense sand, it is possible to assess an average magnitude of the shear strain appropriate to each triangular element. Using these magnitudes in conjunction with a stress ratio shear strain law, a value of mobilised shearing resistance may be defined. Thus ζ, for each element, may be defined for any specific angle of wall rotation by inserting the appropriate values of ϕ_m and ν (ν is assumed constant and equal to 20^0 for dense Leighton Buzzard sand) into Equation 1. In the case of loose sand the empirical relationship $\gamma_M = 1.16 \frac{H\theta}{S}$ and $\nu = 0^0$ have been employed. The angle of the stress vector on those sides of a triangular element which are common to two elements, such as side DH (Fig.20(a)) is defined from the Mohr's circle of stress appropriate to the right hand element for the elements as drawn in Fig.20. The results of a series of calculations using the method outlined briefly above are given in Figs.21 and 22 together with experimental observations.

Fig.21 presents a plot of passive earth pressure coefficient K_p multiplied by sec δ versus angle of wall rotation θ. Fig.22 presents the mobilised angle of wall friction versus θ.

In both diagrams the full lines relate to the theoretical calculations and the broken lines to the observations.

Considering dense sand first, the degree of correlation up to peak between observed and predicted mobilised earth pressure coefficient is good. The correlation beyond peak is poor, i.e. portions of the curves PQ and PR are quite unrelated; however, this may have been anticipated since beoyond peak it is known that strong discontinuities form within the sand mass and hence

the empirical strain relationship ($\gamma_M = 1.47 \frac{H\theta}{S}$) employed for dense sand is no longer applicable. When such strong discontinuities form the strains become very large and the mobilised shearing resistance will quickly drop to the critical state value.

To some extent the good agreement between the theory and experiment over curve portions $\dot{O}P$ must be considered fortuitous since it is known that the experimentally determined passive earth pressure coefficients include the effects of tank side friction. Nevertheless, in view of the magnitude of the assumptions made and the simplicity of the calculation procedure the degree of correlation is encouraging.

Considering the results for loose sand the degree of correlation at large angles of wall rotation is good but deteriorates in the early stages of wall movement. In this case one would expect good correlation at peak since strong discontinuities do not form at large wall rotations. However, poorer correlation would be expected at the smaller angles of wall movement since it is known that the loose sand suffers substantial contraction during the early stages of shear deformation (i.e. $\nu < 0$), whereas for simplicity in the loose calculations ν was assumed equal to zero. The corresponding mobilised angle of wall friction data presented in Fig.22 indicate a good correlation for the loose sand and a much less satisfactory correlation for the dense sand.

CONCLUDING REMARKS

My primary objectives in this paper have been to classify model testing dependent upon the immediate goals of the tests, and to indicate the value of the more academic Category III test. It

was stated that Category I tests, in general, are difficult to perform within the laboratory due to problems associated with modelling the soil. However, centrifugal model testing is expected to increase the attraction of this type of test since it allows the use of prototype soils at prototype stress levels.

From the point of view of advancing our knowledge and developing new and better methods of analysis Category II and Category III tests offer the most profitable approach. In the long term it is anticipated that finite element analysis employing laboratory determined soil parameters will be able to give accurate predictions of the behaviour of complex full scale prototype structures; however before that day can arrive model testing has a vital role to perform by providing data for detailed comparison between prediction and reality.

In the latter part of the paper it was shown how a Category III type experiment could shed light on the phenomena of progressive failure. Subsequently an empirical approach to predict the load displacement relationship for the problem considered was made. The results illustrate the limitations of the simple approach; however they also illustrate the importance of taking strains into consideration. There is a serious gap in our theoretical and experimental knowledge of the kinematic behaviour in soils problems which urgently needs to be filled. There are numerous static stress field solutions to soils problems which employ a constant ϕ idealisation, but such solutions usually take no account of the kinematics or the effects of strains (see Davis (1968)). There are precious few complete kinematic solutions and solutions which satisfy kinematic considerations, static stress

field requirements and the real stress strain laws of soil are almost unknown. Only when all three requirements are satisfied simultaneously will satisfactory load displacement predictions be possible.

Thus a more detailed theoretical and experimental study of soil kinematics, via Category III type experimentation, is likely to prove a rewarding and valuable exercise.

ACKNOWLEDGEMENTS

The author wishes to acknowledge a debt of gratitude to the late Professor Roscoe for his continuous inspiration and encouragement over the last decade. It was both a pleasure and a privilege to work as a member of his research team. I am sure that by continued perseverance we may ultimately achieve the goals that Ken Roscoe pursued in such a dedicated fashion. I also wish to extend my thanks to all the members of the Cambridge Soil Mechanics group and Engineering Department who have assisted me in preparation of this paper.

REFERENCES

BUTTERFIELD R., HARKNESS R.M., & ANDRAWES K.Z. (1970) "A stereo-photogrammetric method for measuring displacement fields." Géotechnique 20:3:308-314.

DAVIS E.H. (1968) "Theories of plasticity and the failure of soil masses." Soil Mechanics Selected Topics, Ed.K.I.Lee, Butterworths.

ENDICOTT L.J. (1971) "Centrifugal testing of soil models." Ph.D.Thesis, Cambridge University.

HANSEN, J.Brinch (1953) "Earth pressure calculations." Danish Technical Press, pp 271.

JAMES R.G. (1965) "Stress and strain fields in sand." Ph.D.Thesis, Cambridge University.

JAMES R.G. & BRANSBY P.L. (1971) "A velocity field for some passive earth pressure problems." Géotechnique 21:

LEUSSINK H., BLINDE A., & ABEL P. (1966) "Versuche über die sohldruckverteilung unter starren Gründungs Köppern auf Kohärsionlosens Sand." Veröffentlichungen des Institutes für Bodenmechanik und Felsmechanik der Technischen Hochschule Fridericiana Universität Karlsruhe.

LORD J.A. (1969) "Stresses and strains in an earth pressure problem." Ph.D.Thesis, Cambridge University.

LYNDON A. & SCHOFIELD A.N. (1970) "Centrifugal model test of a short-term failure in London clay." Technical Note Géotechnique 20:4:440-442.

ROCHA M. (1957) "The possibility of solving soil mechanics problems by the use of models." Proc.4th Int.Conf. Soil Mech., London, I:183.

ROSCOE K.H. (1968) "Soils and model tests." Journal of Strain Analysis Vol.3:1:57-64.

ROSCOE K.H. (1970) "The influence of strains in soil mechanics." 10th Rankine Lecture, Géotechnique 20:2:129-170.

ROWE P.W. & PEAKER K. (1965) "Passive earth pressure measurements Geotechnique 15:1:57.78.

SKEMPTON A.W. & HUTCHINSON J. (1969) "Stability of natural slopes and embankment foundations." State of the Art Volume, Proc. 7th Int.Conf.Soil Mech & Found.Eng., Mexico, 291-340.

SUTHERLAND H.B. (1965) "Model studies for shaft raising through cohesionless soils." Proc.6th Int.Conf.Soil Mech., Montreal, II:410-413.

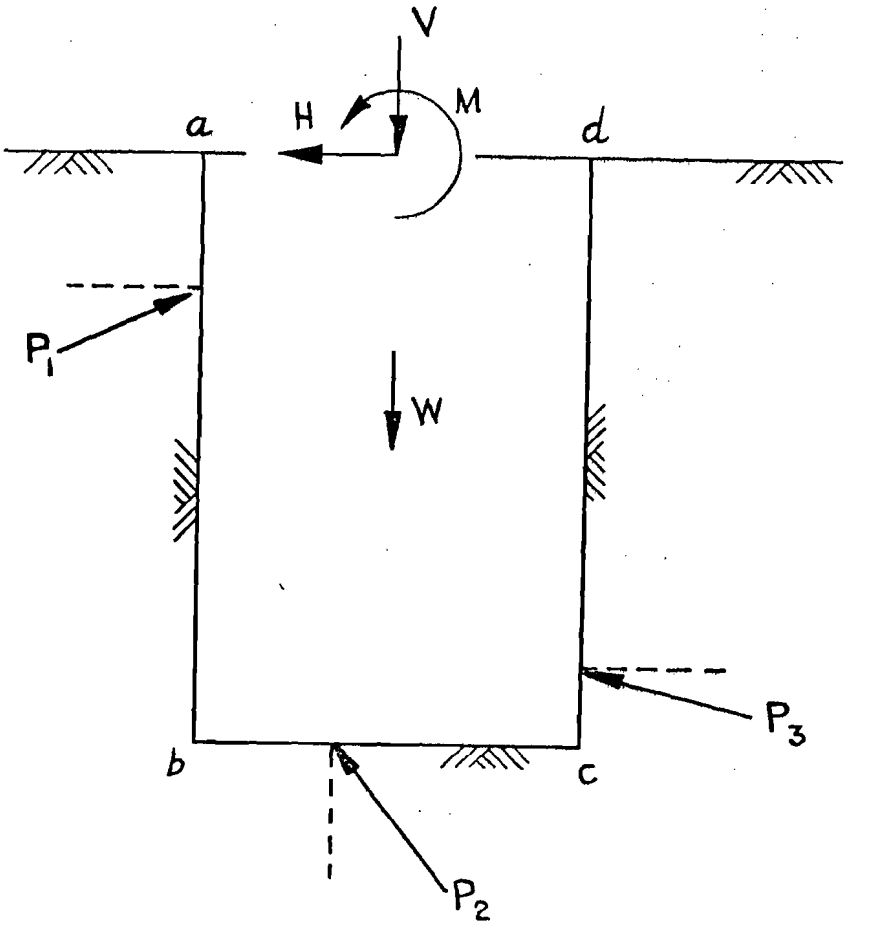

FIG. 1. THE GENERAL 2-DIMENSIONAL PROBLEM.

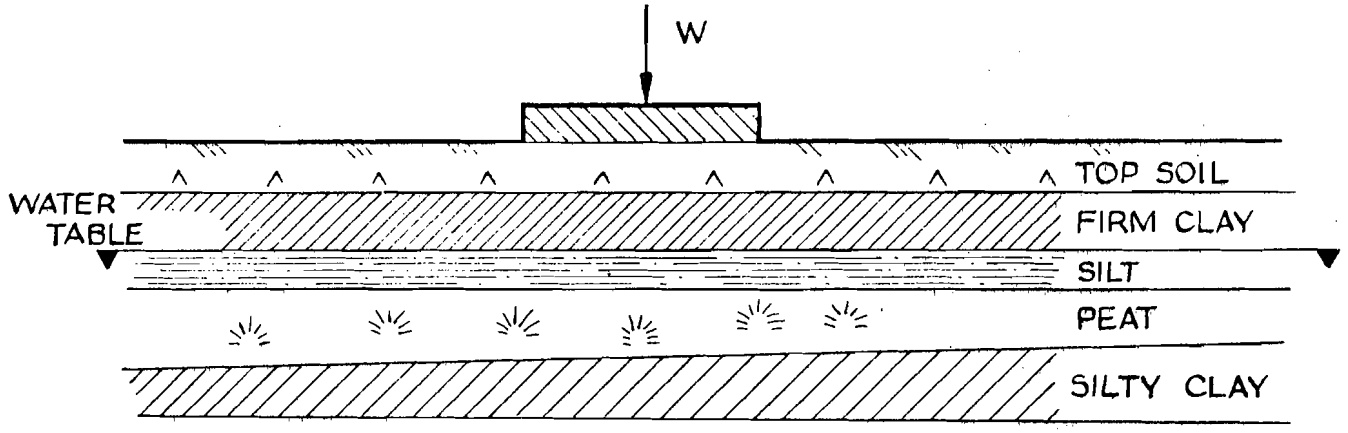

(a) CATEGORY I TEST SIMULATING REAL PROTOTYPE

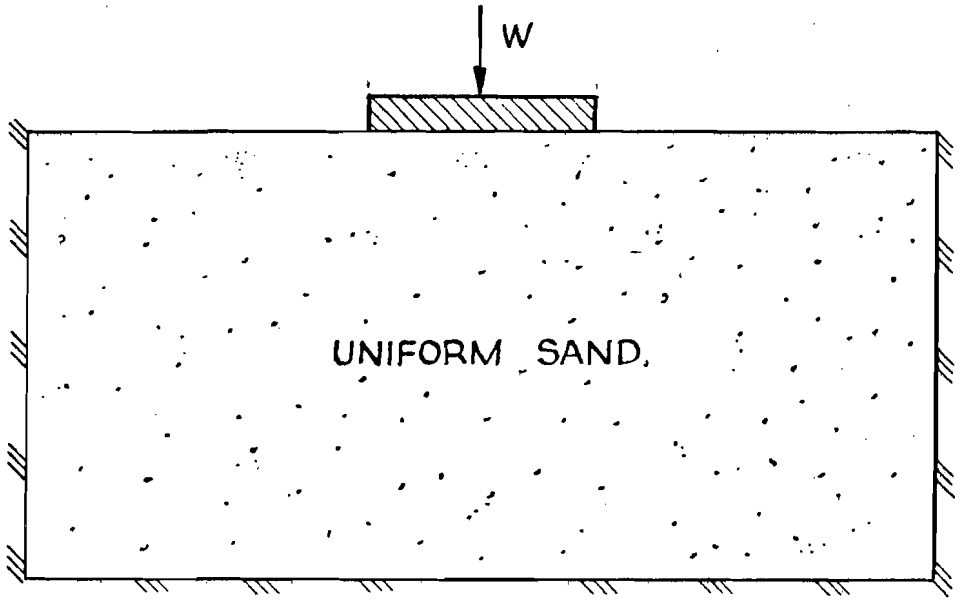

(b) CATEGORY II TEST IDEALIZED SMALL PROTOTYPE

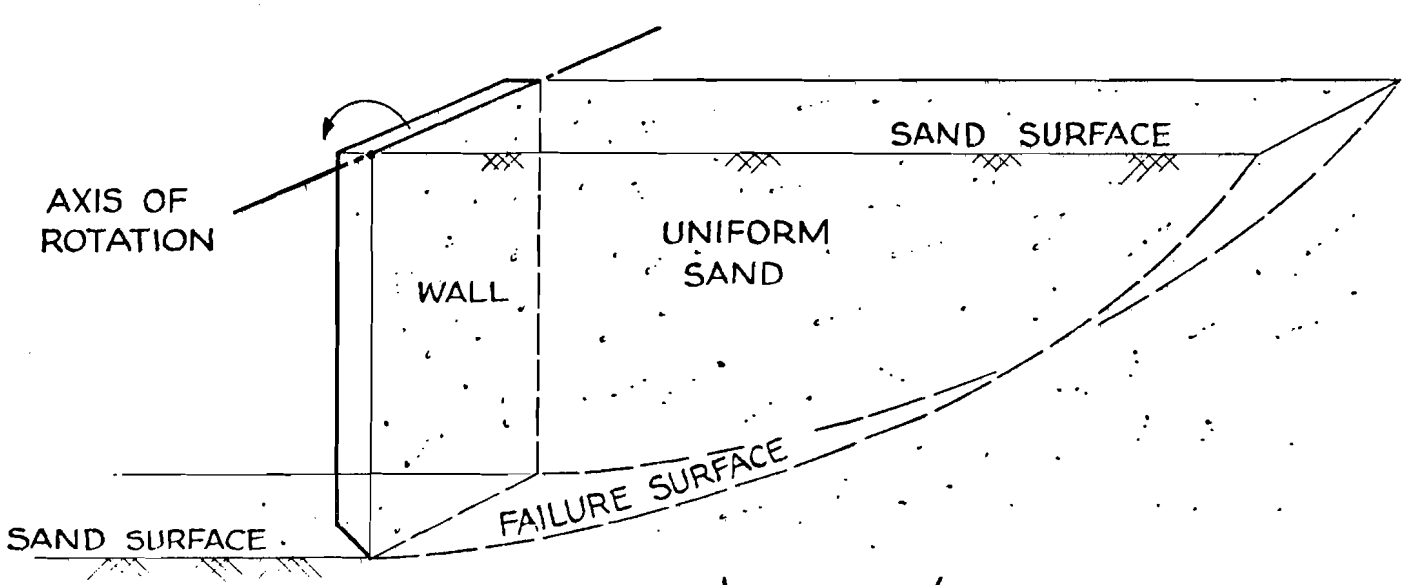

(c) CATEGORY III TEST IDEALISED 'ARTIFICIAL' PROTOTYPE

FIG. 2 MODEL TEST CATEGORIES.

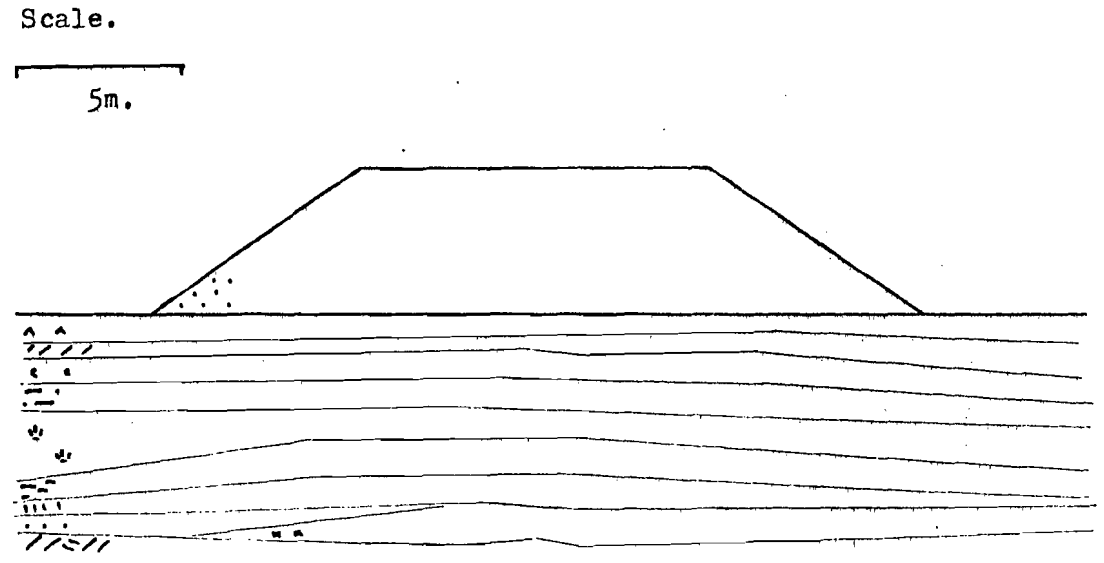

Key to soils:

- embankment fill
- topsoil
- firm brown clay
- soft brown clay
- soft grey silty clay
- peat
- soft blue silty clay
- soft dark silty clay
- blue sand
- firm blue clay
- weathered Kimmeridge Clay

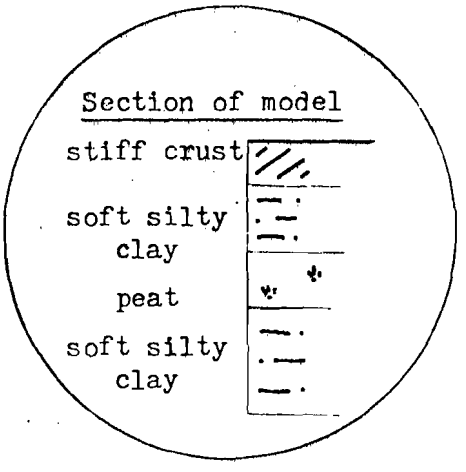

Figure.3. Soil strata beneath trial embankment at King's Lynn

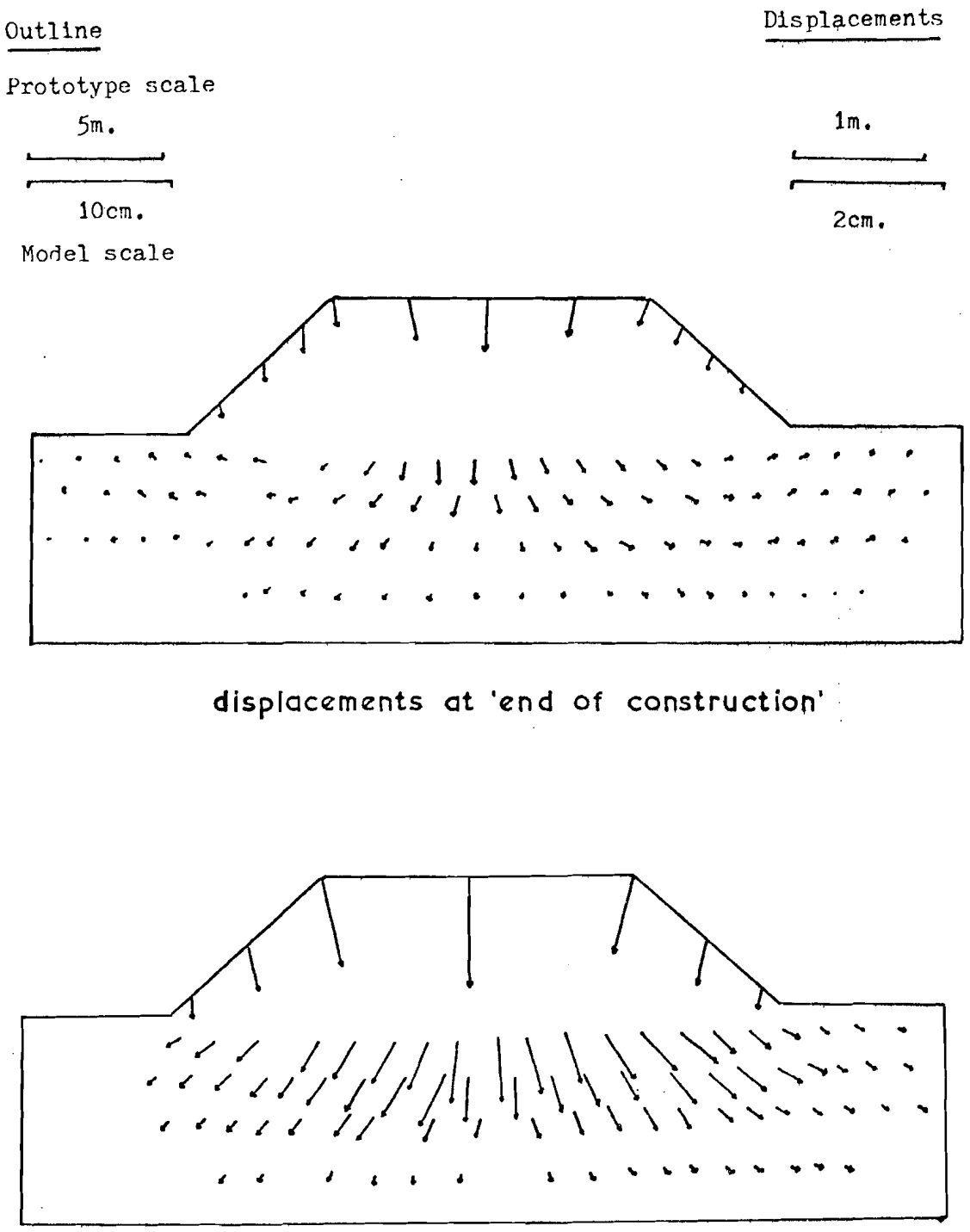

Figure.4. Displacements of model of the trial embankment

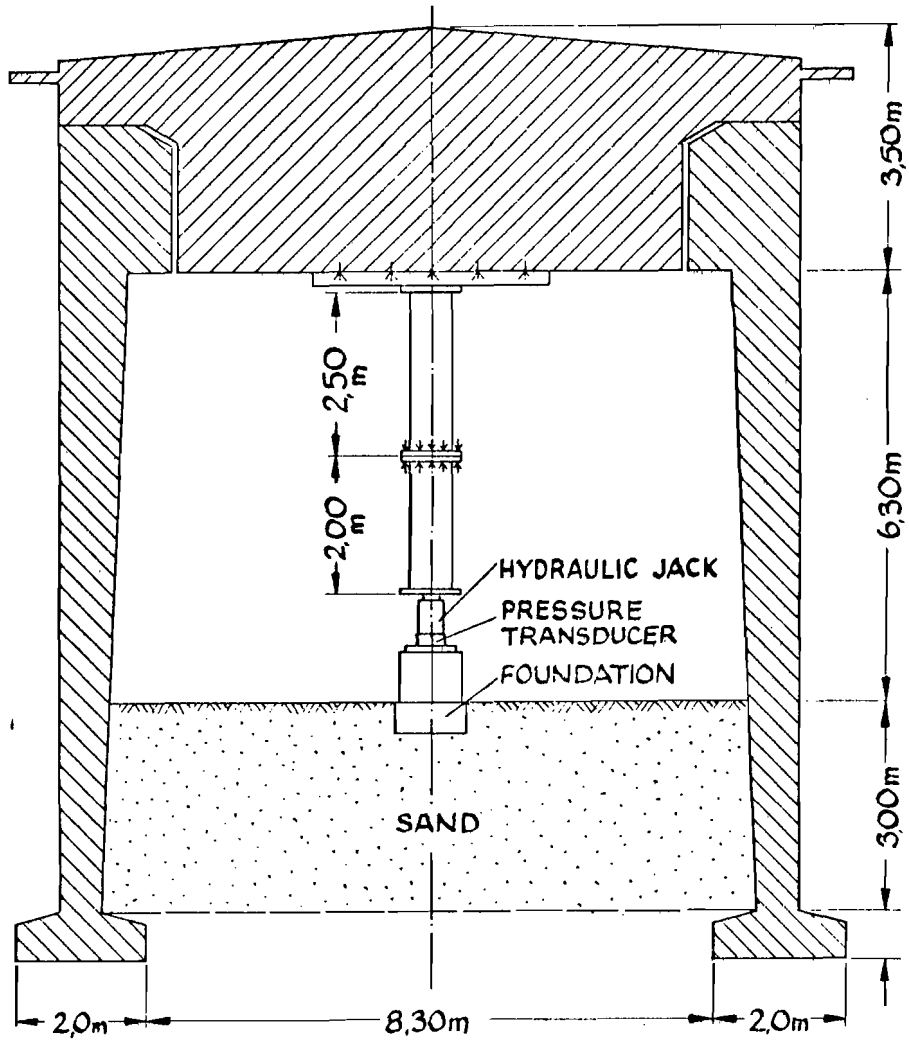

FIG. 5 KARLSRUHE UNIVERSITY LARGE FOOTING APPARATUS

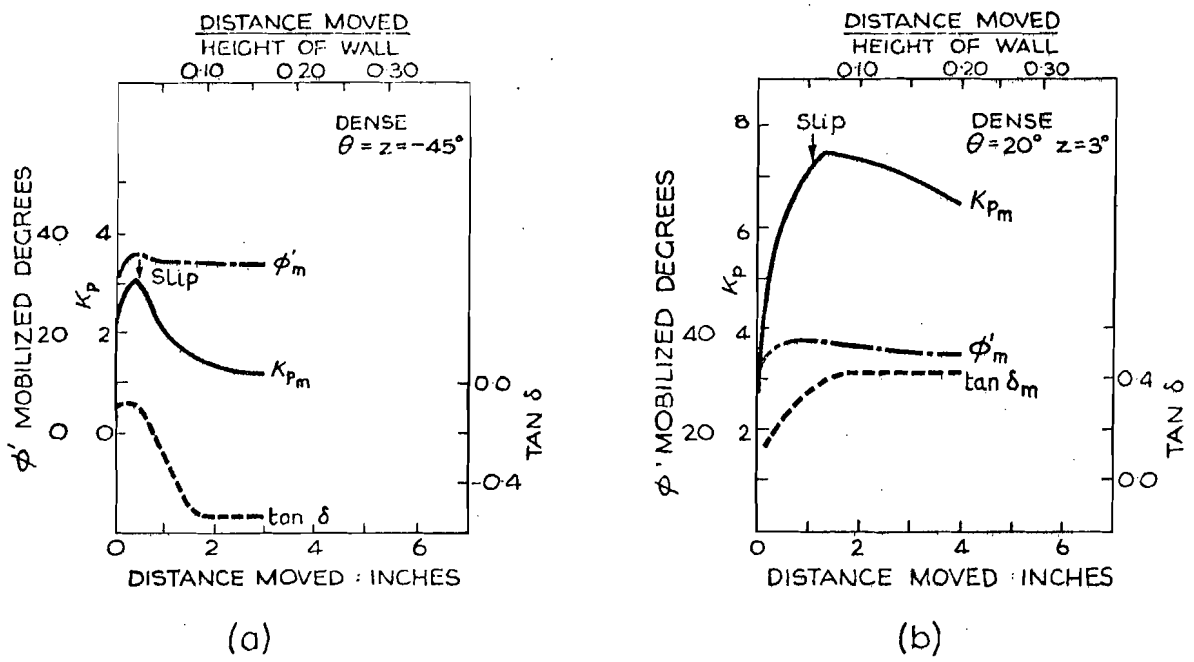

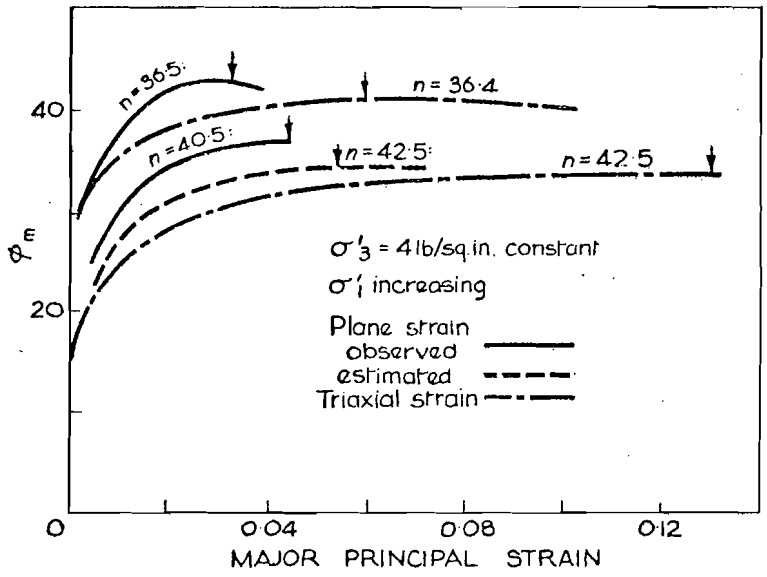

(c) ϕ'_m - STRAIN CURVES FOR LOOSE AND DENSE SAND IN THE TRIAXIAL AND PLANE STRAIN TESTS

FIG. 6 PASSIVE EARTH PRESSURE RESULTS FROM ROWE & PEAKER 1965

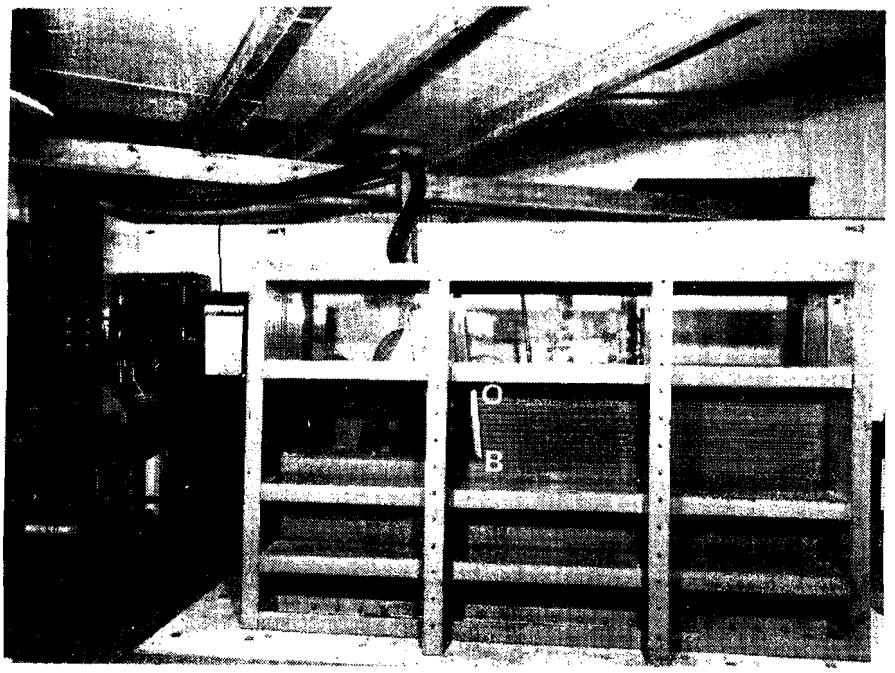

Fig.7. Model earth pressure apparatus and recording equipment showing instrumented wall OB.

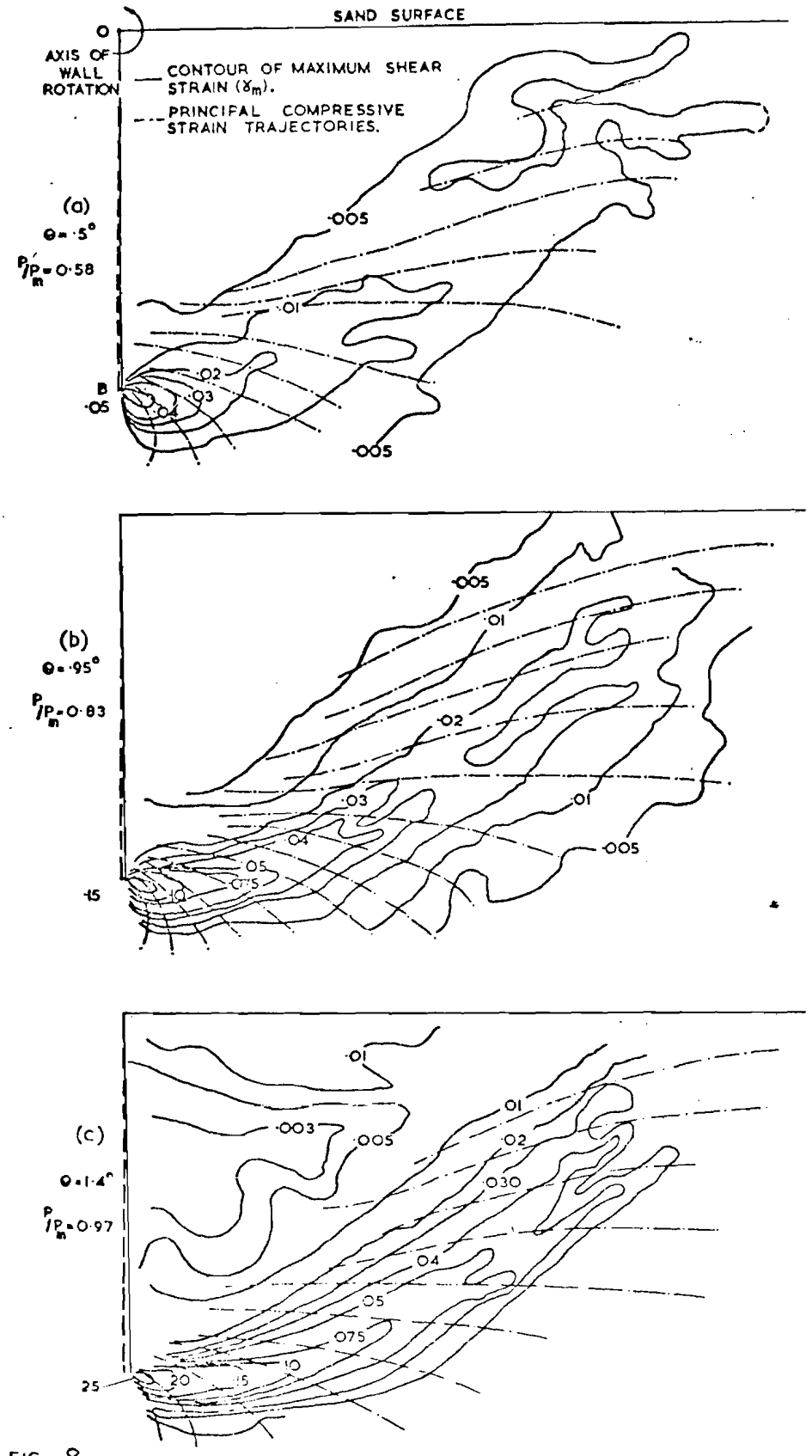

FIG. 8. CUMULATIVE SHEAR STRAINS AND PRINCIPAL COMPRESSIVE STRAIN TRAJECTORIES FOR TEST L E (ϵ_0=0·550) JAMES 1965.

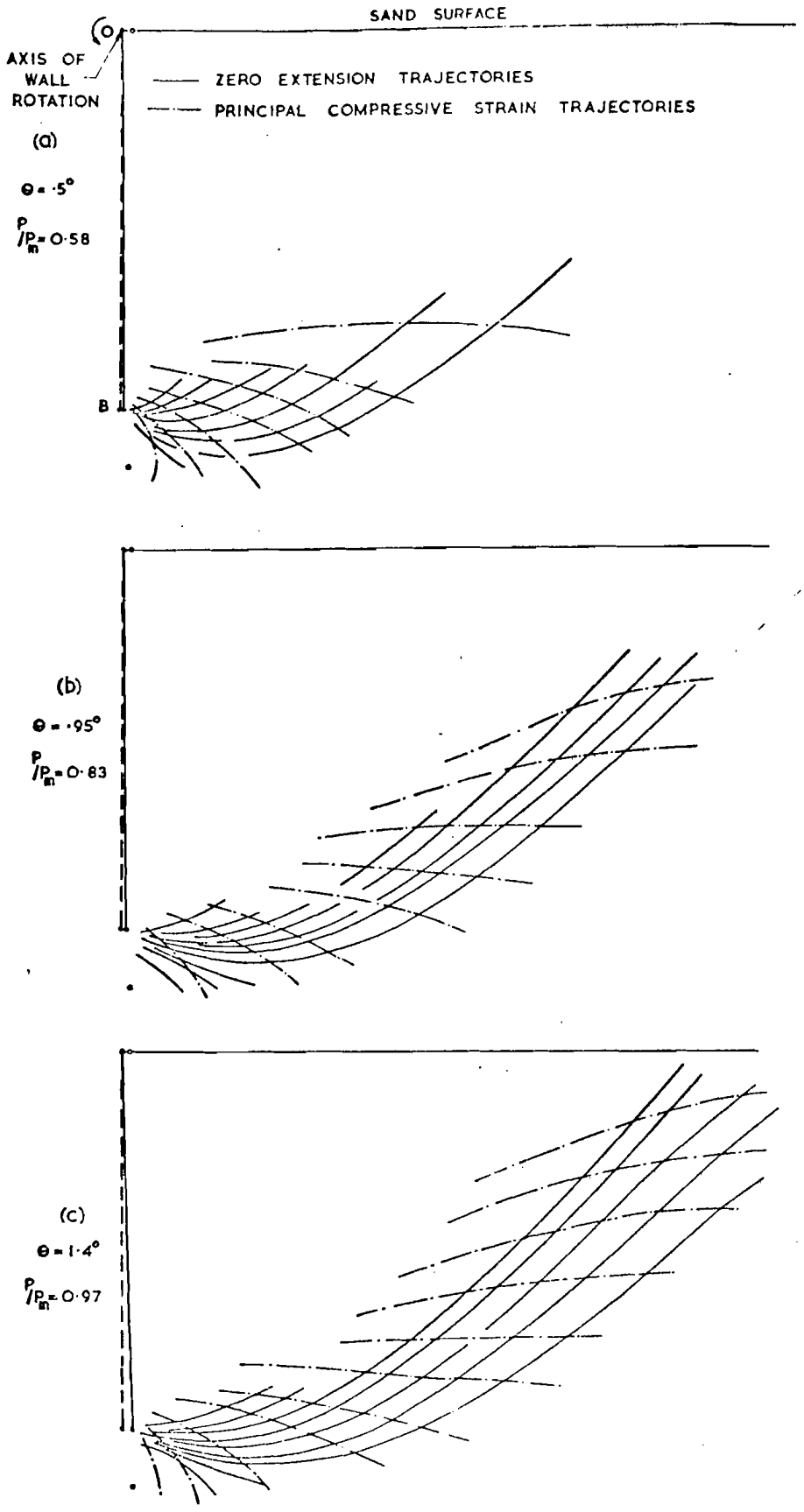

FIG. 9. TRAJECTORIES OF ZERO EXTENSION AND PRINCIPAL COMPRESSIVE STRAIN FOR TEST LE (e_o = 0·550) JAMES 1965.

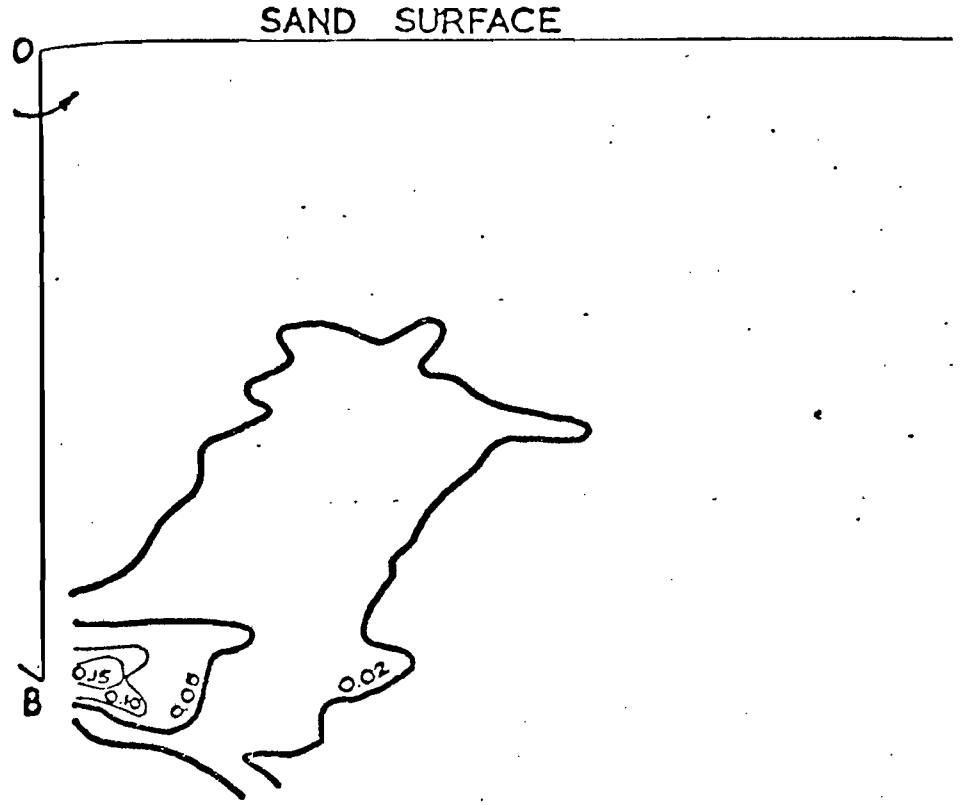

MAX. SHEAR STRAIN 0.159

(a) INCREMENT Nº 1 $\theta = 0 \rightarrow 1°$

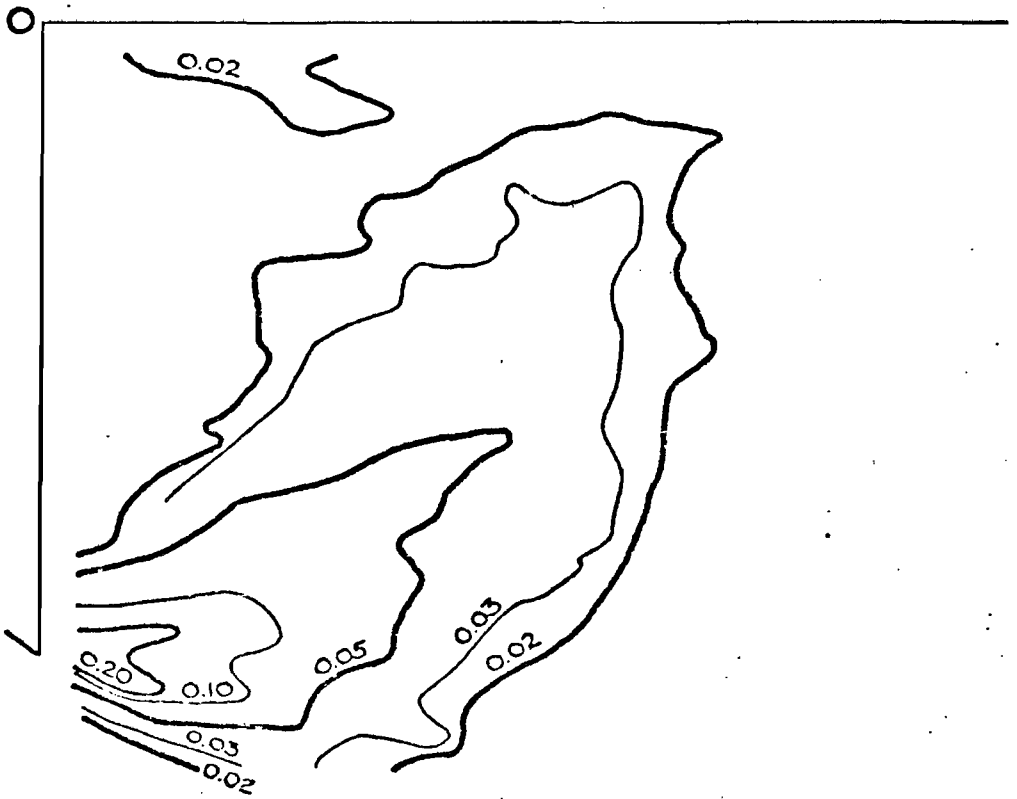

MAX. SHEAR STRAIN 0.357

(b) CUMULATIVE STRAINS AT $\theta = 2°$

FIG. 10. CUMULATIVE SHEAR STRAINS FOR TEST MD (e_o: 0·70) LORD 1969

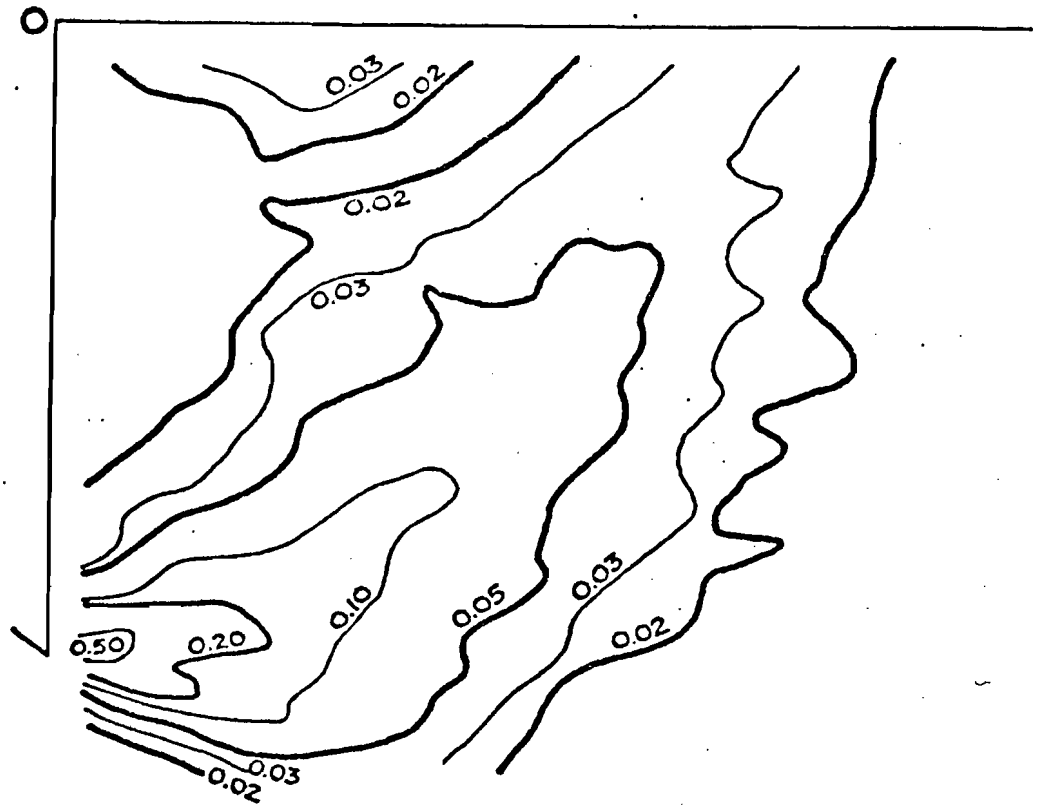

MAX. SHEAR STRAIN 0.573

(c) CUMULATIVE STRAINS AT $\theta = 3°$

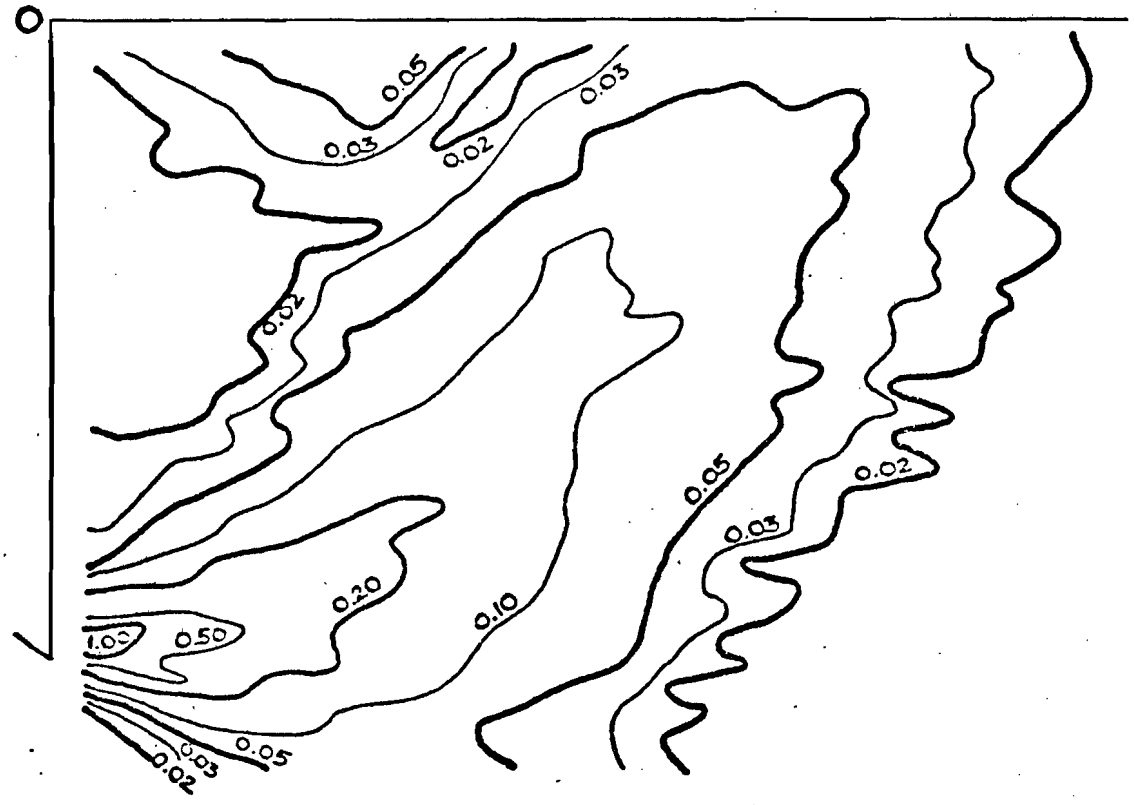

MAX. SHEAR STRAIN 1.183

(d) CUMULATIVE STRAINS AT $\theta = 5°$

FIG. 10. CUMULATIVE SHEAR STRAINS FOR TEST MD

e_o : 0·70 LORD 1969

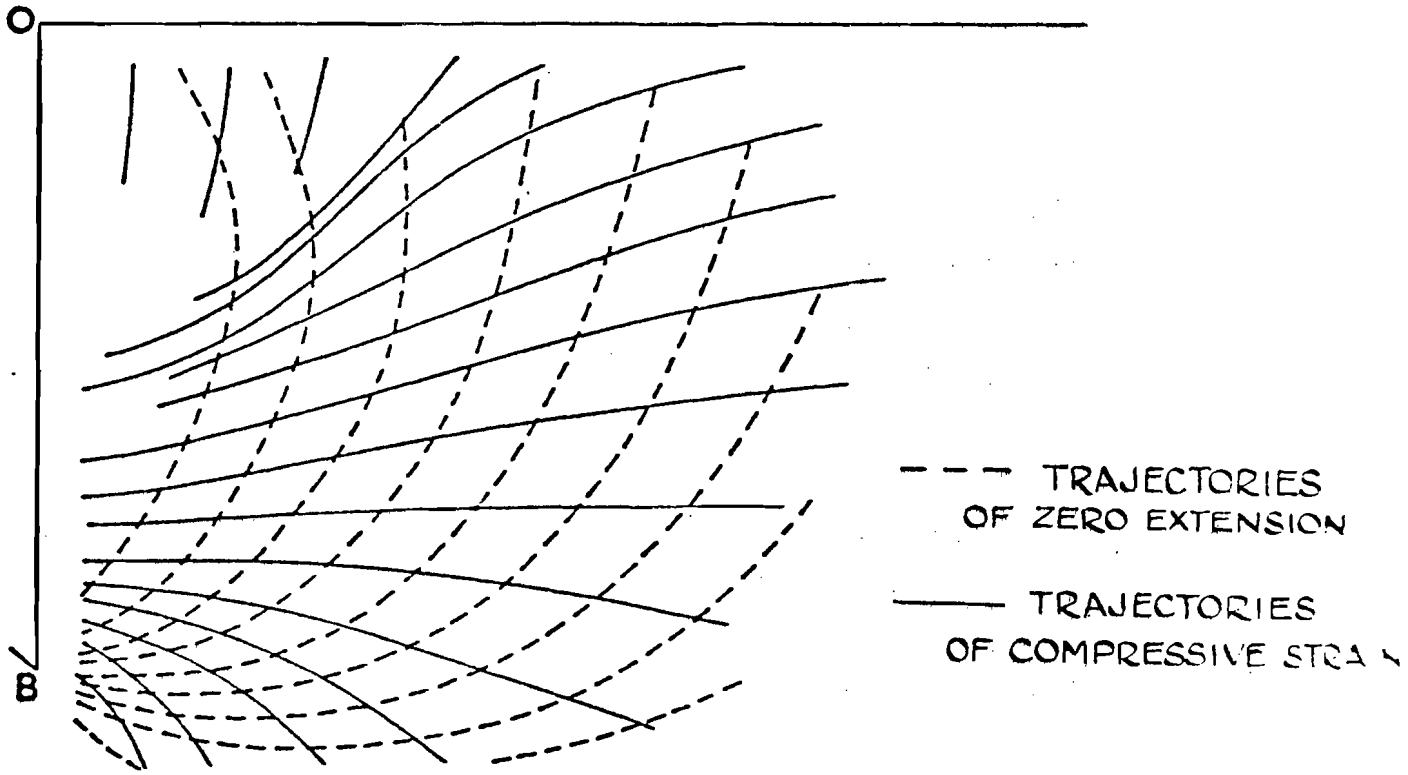

(a) BASED ON CUMULATIVE STRAINS AT $\theta = 2°$

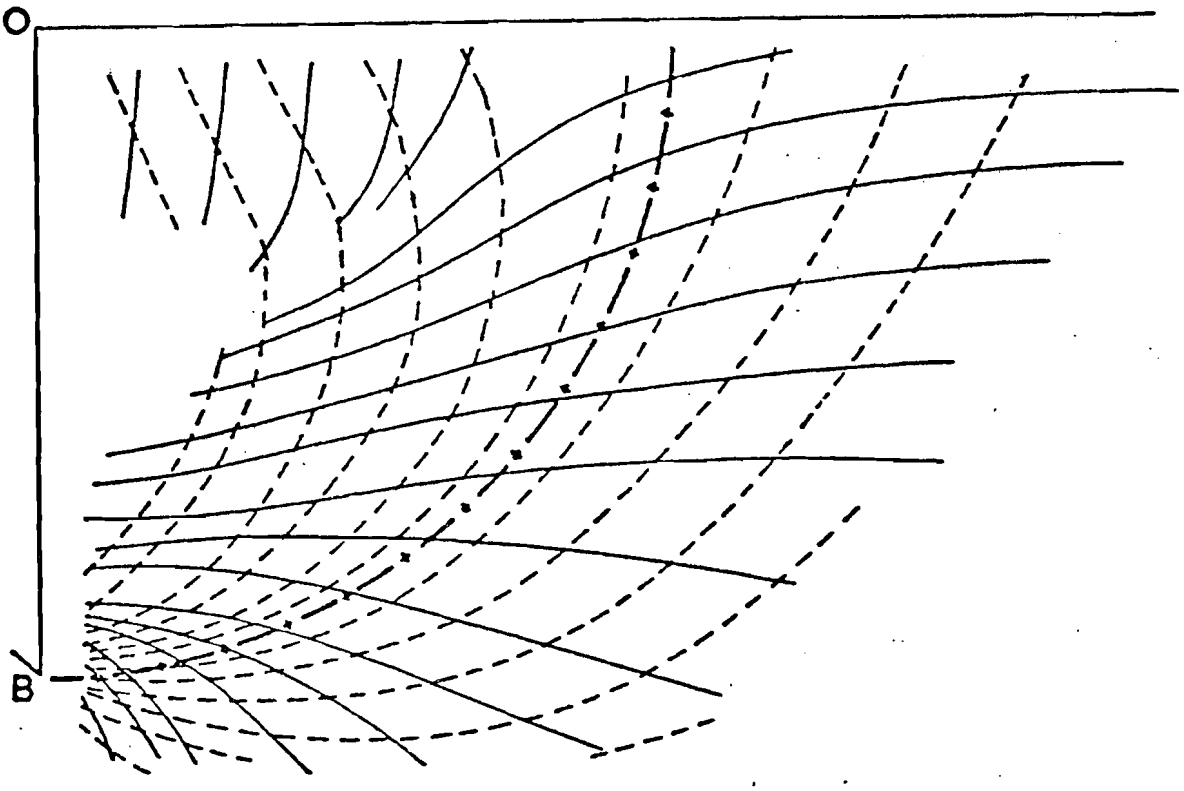

(b) BASED ON CUMULATIVE STRAINS AT $\theta = 5°$

FIG. 11. TRAJECTORIES OF ZERO EXTENSION AND PRINCIPAL COMPRESSIVE STRAIN. TEST M.D. ($e_o = 0{\cdot}70$) LORD 1969

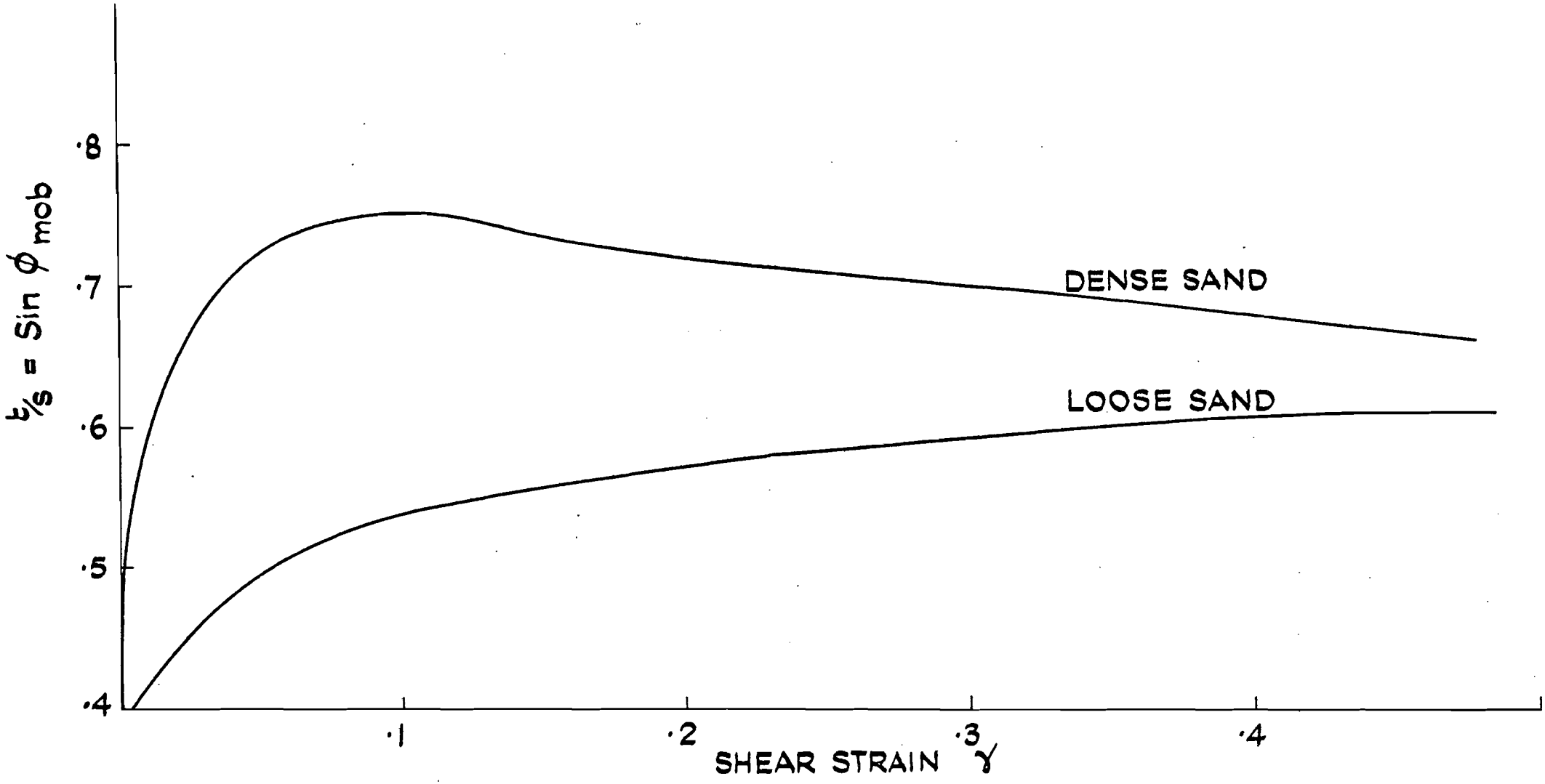

FIG. 12. TYPICAL STRESS RATIO STRAIN RELATIONSHIPS FOR SAND FROM THE SIMPLE SHEAR APPARATUS.

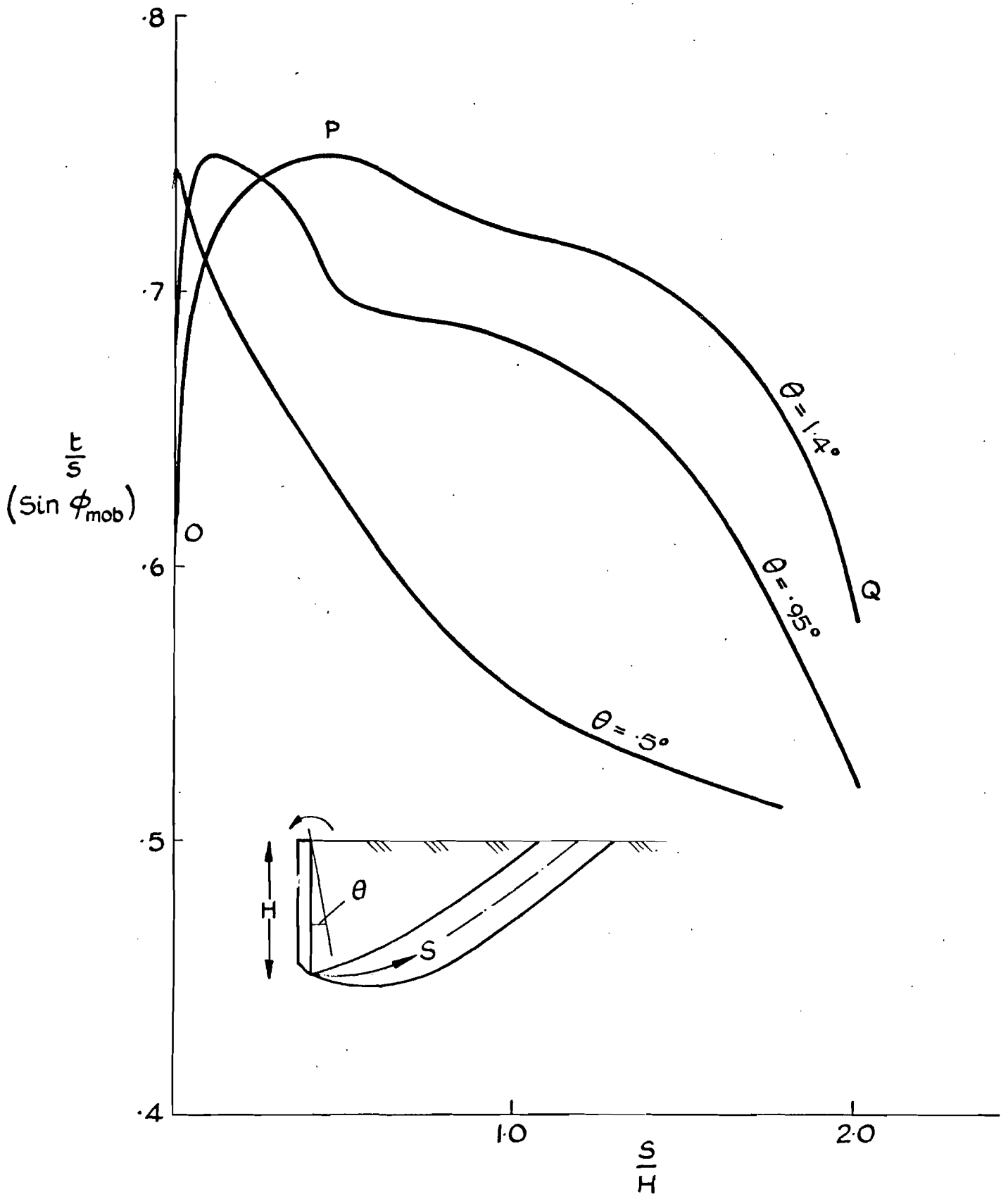

FIG. 13 MOBILIZED SHEAR STRENGTH DISTRIBUTIONS ALONG CENTRE LINE OF TRANSITION LAYER FOR TEST. LE ($l_o = ·55$)

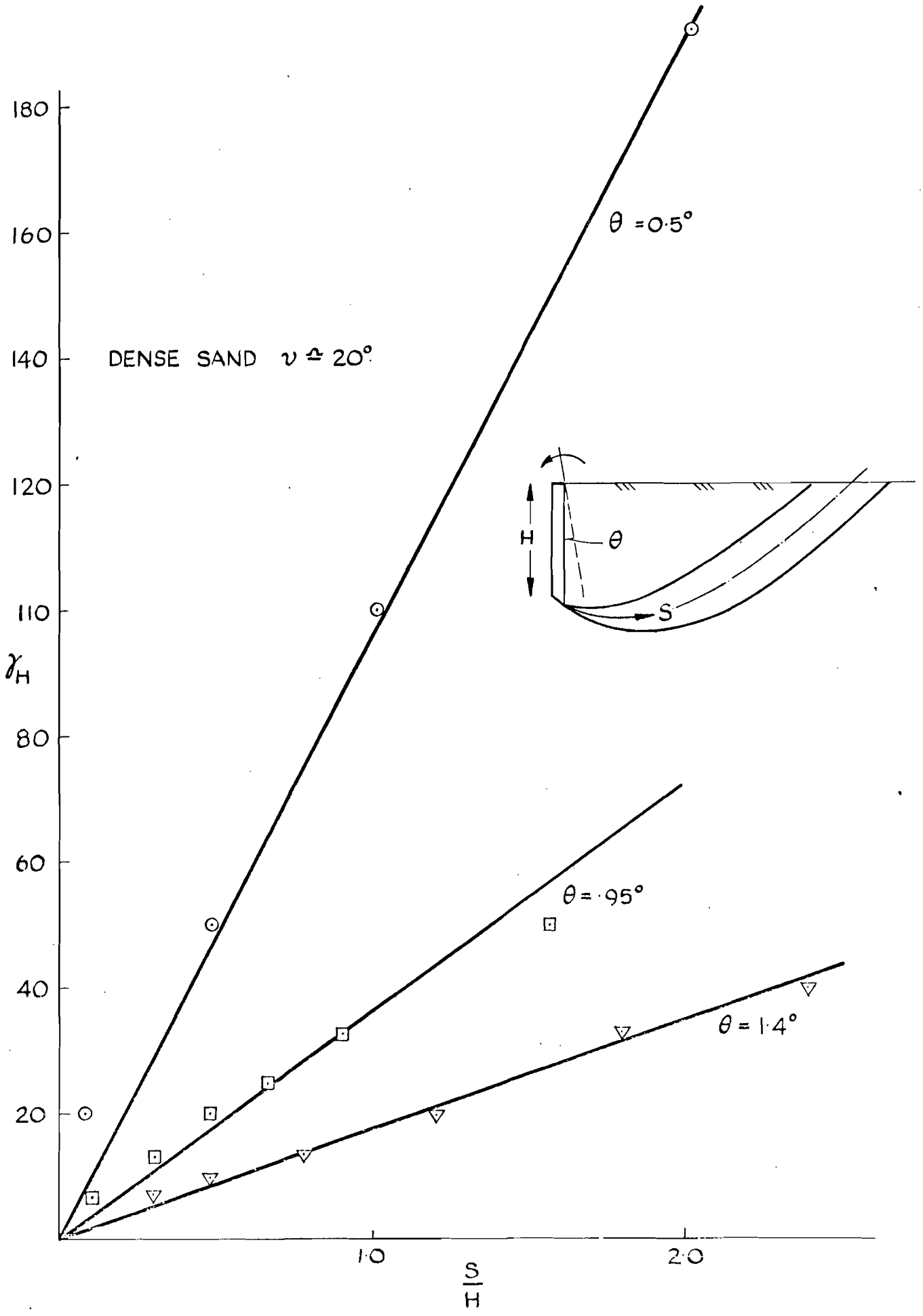

FIG. 14 SHEAR STRAIN RELATIONSHIPS ON THE CENTRE LINE OF THE TRANSITION LAYER FOR TEST. LG (ℓ_0 = ·55)

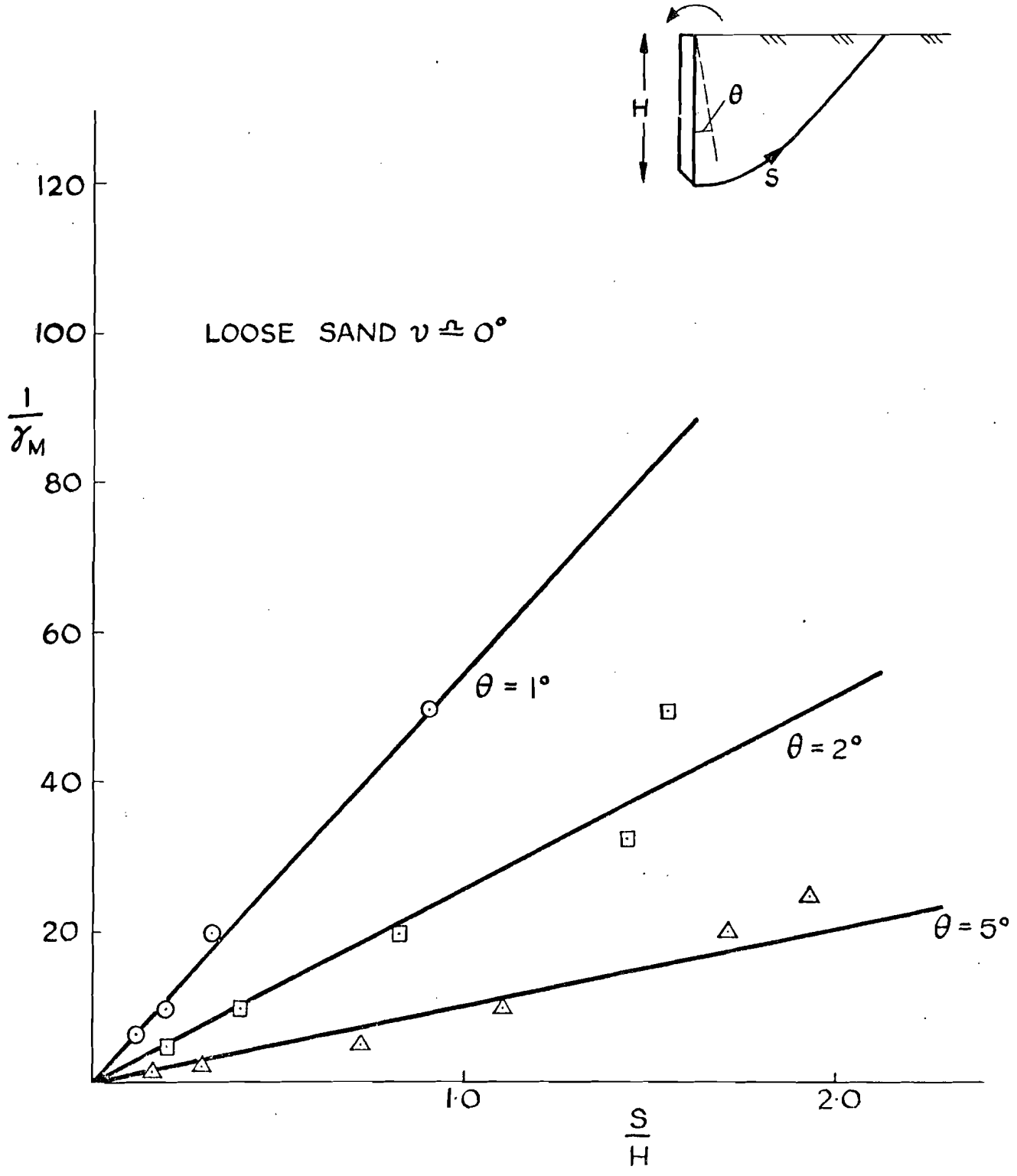

FIG.15 SHEAR STRAIN RELATIONSHIPS ON CENTRE LINE OF TRANSITION LAYER FOR TEST. M D ($\ell_o = 0{\cdot}70$)

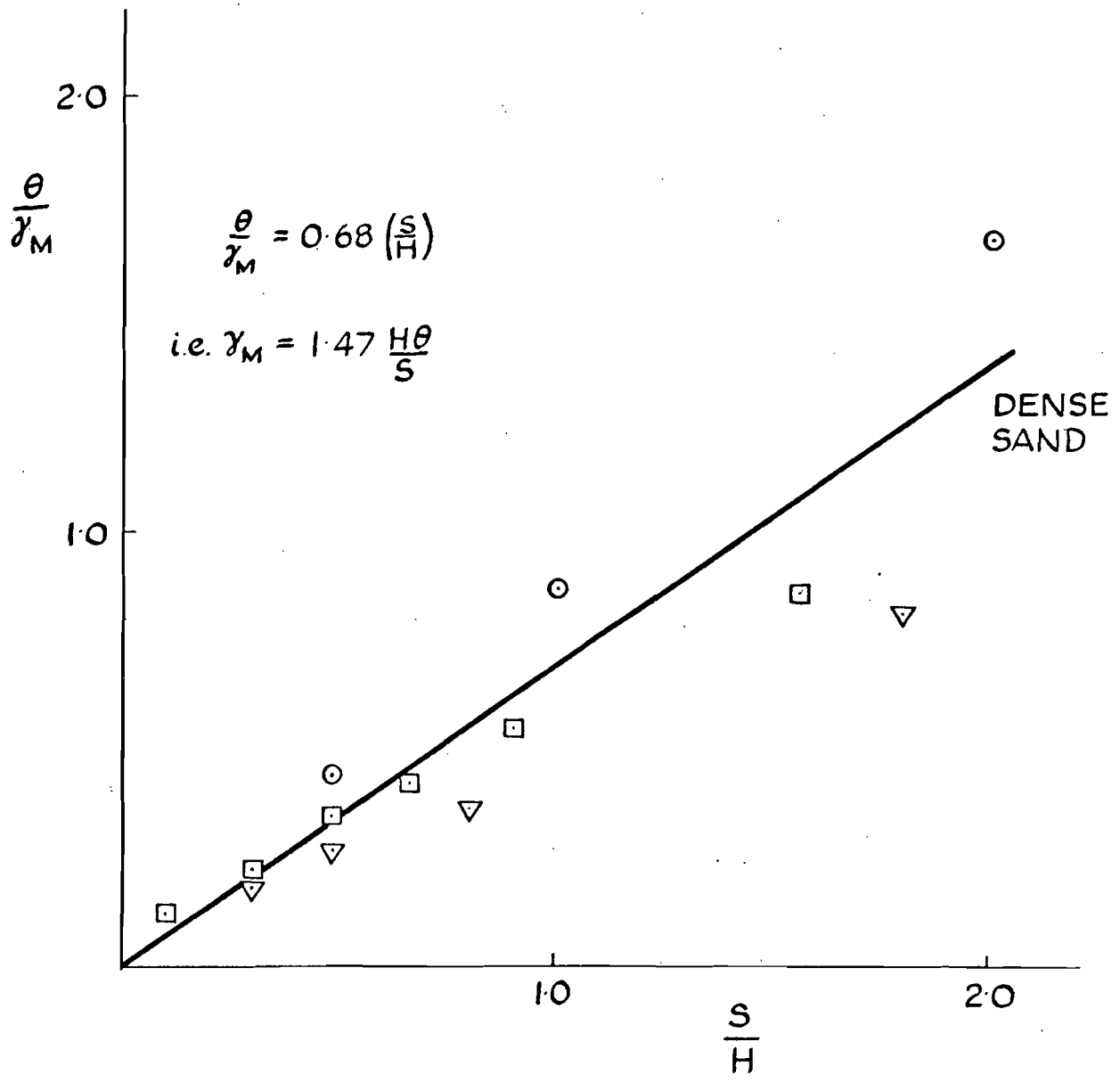

FIG. 16 SHEAR STRAIN RELATIONSHIP ON CENTRE LINE OF TRANSITION LAYER FOR TEST. L E (ℓ_o = ·55)

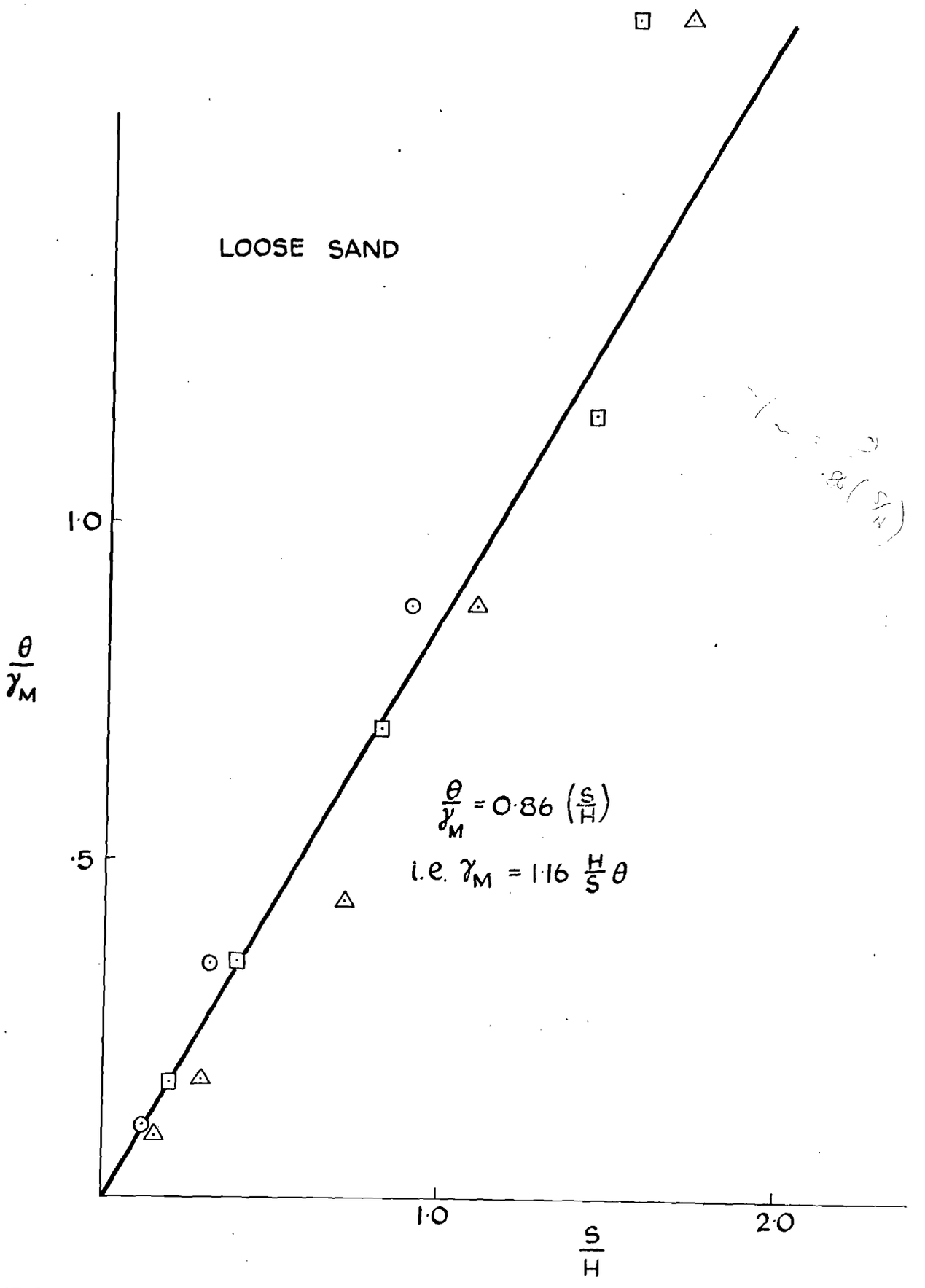

FIG. 17 SHEAR STRAIN RELATIONSHIP ON CENTRE LINE OF TRANSITION LAYER TEST. MD ($\ell_0 = 0{\cdot}70$)

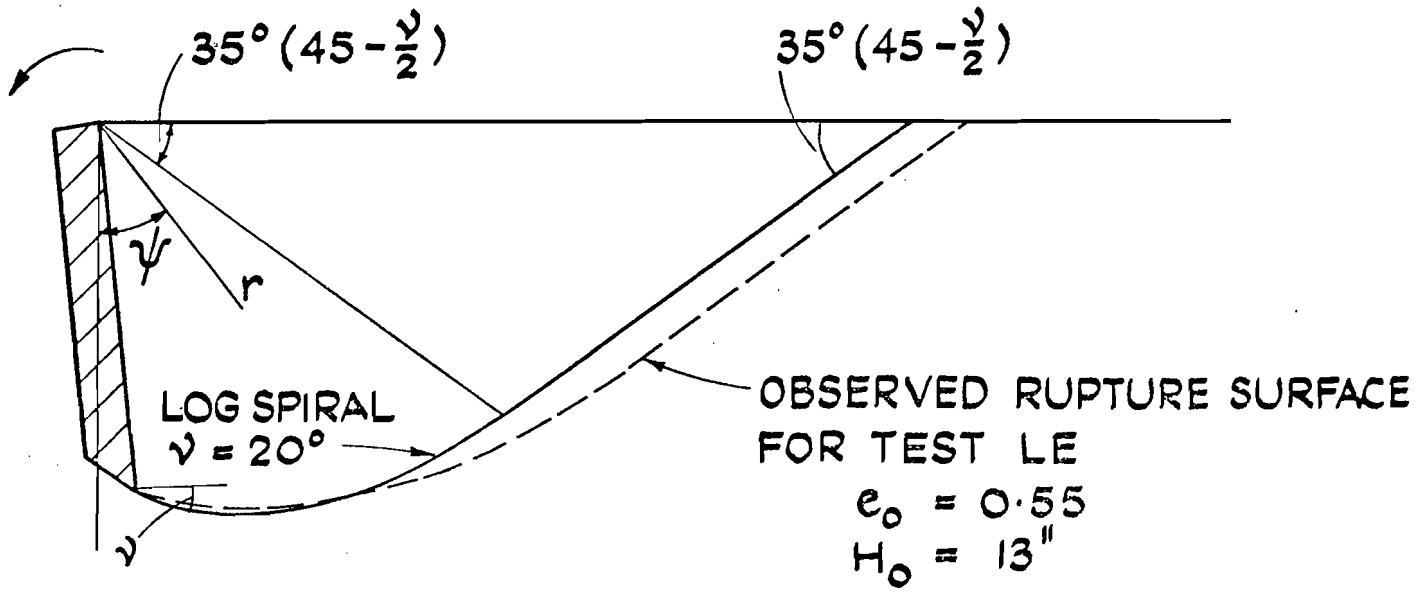

FIG. 18. PREDICTED RUPTURE SURFACE MECHANISM AND AN OBSERVED RUPTURE MECHANISM (JAMES 1965) IN DENSE SAND FOR WALL ROTATION ABOUT THE TOP.

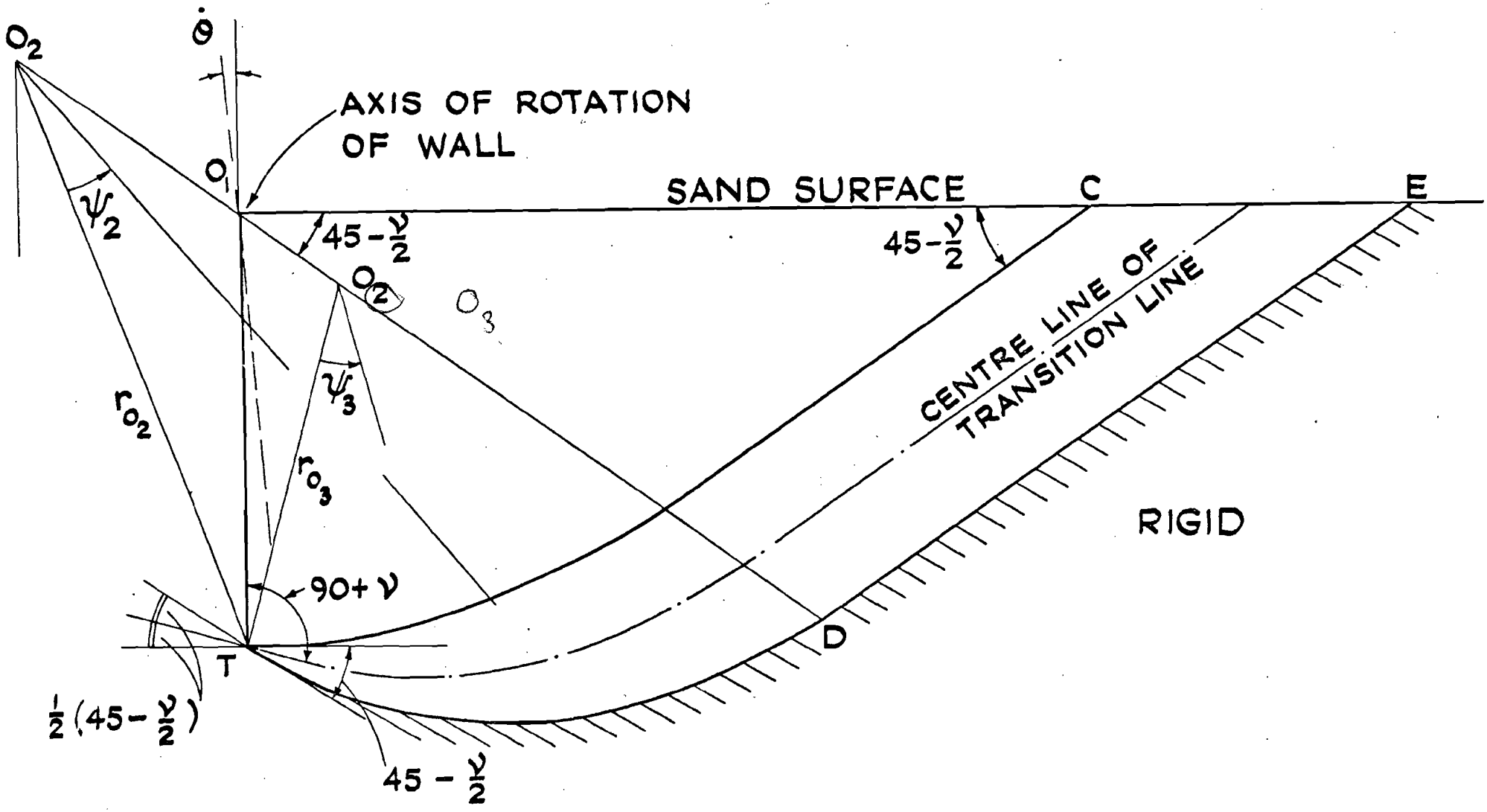

FIG. 19. GEOMETRIC CONSTRUCTION OF THE TRANSITION ZONE FOR A CONSTANT ν MATERIAL.

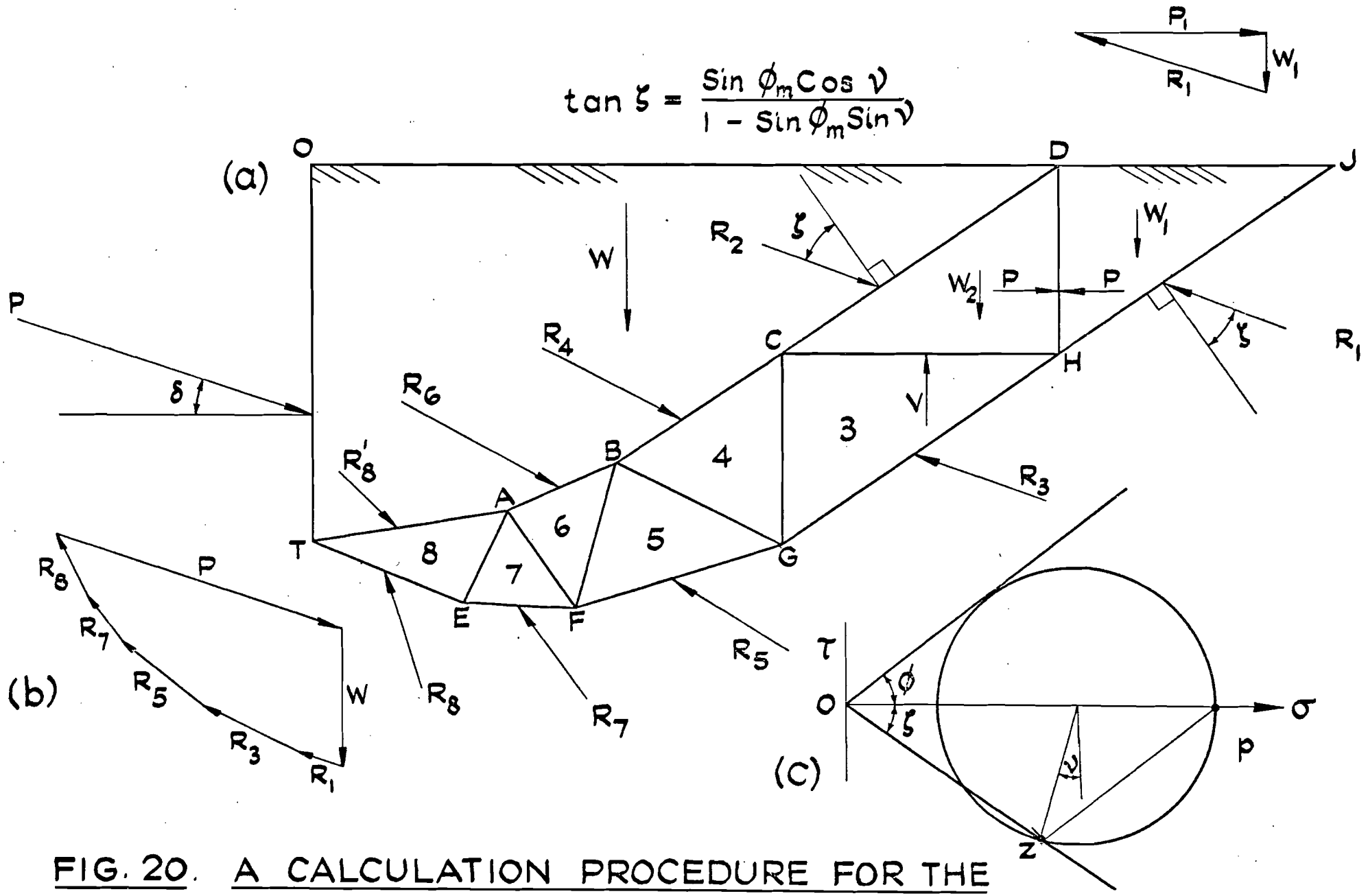

FIG. 20. A CALCULATION PROCEDURE FOR THE DETERMINATION OF PASSIVE EARTH PRESSURE.

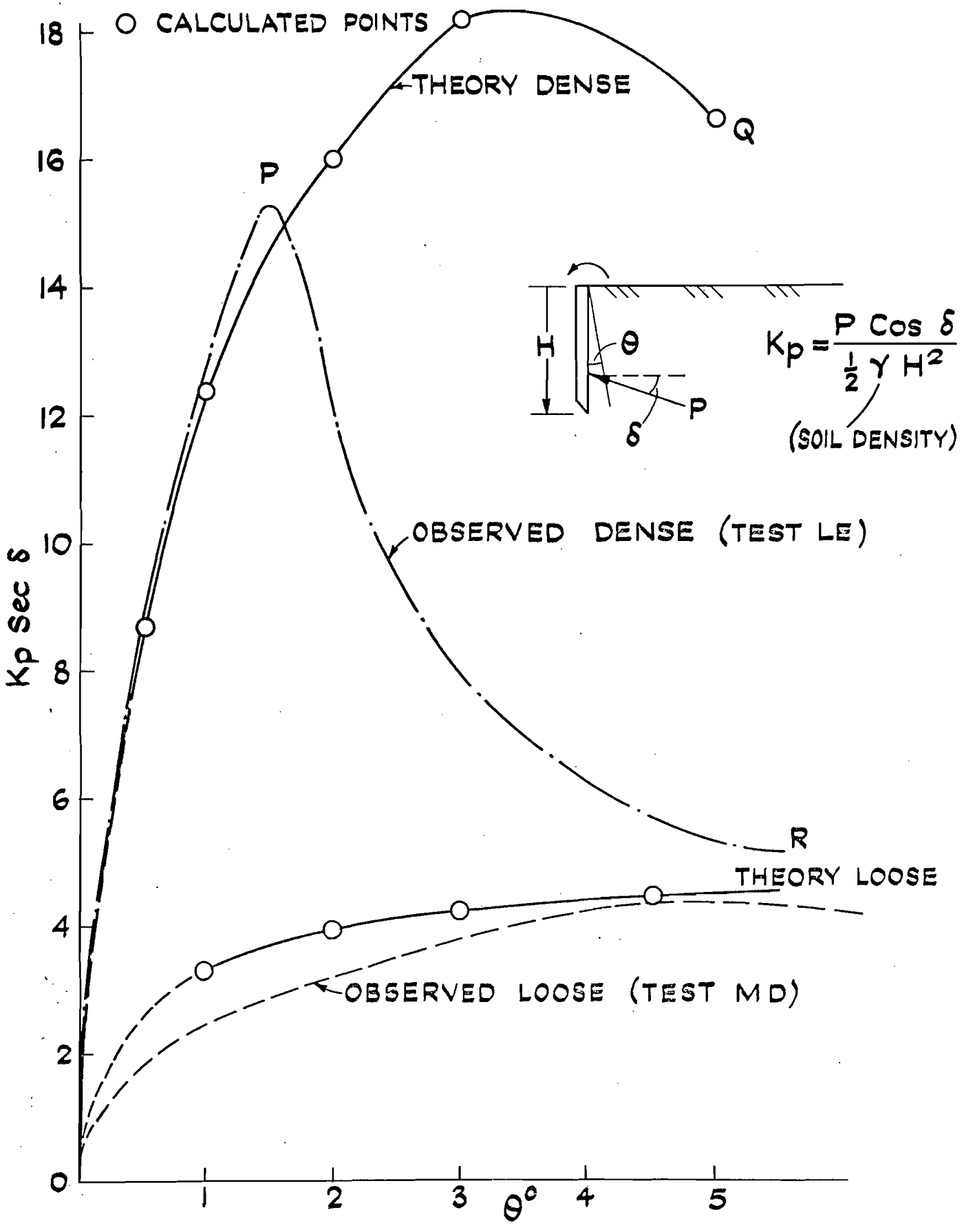

FIG. 21. PASSIVE EARTH PRESSURE - WALL ROTATION RELATIONSHIPS.

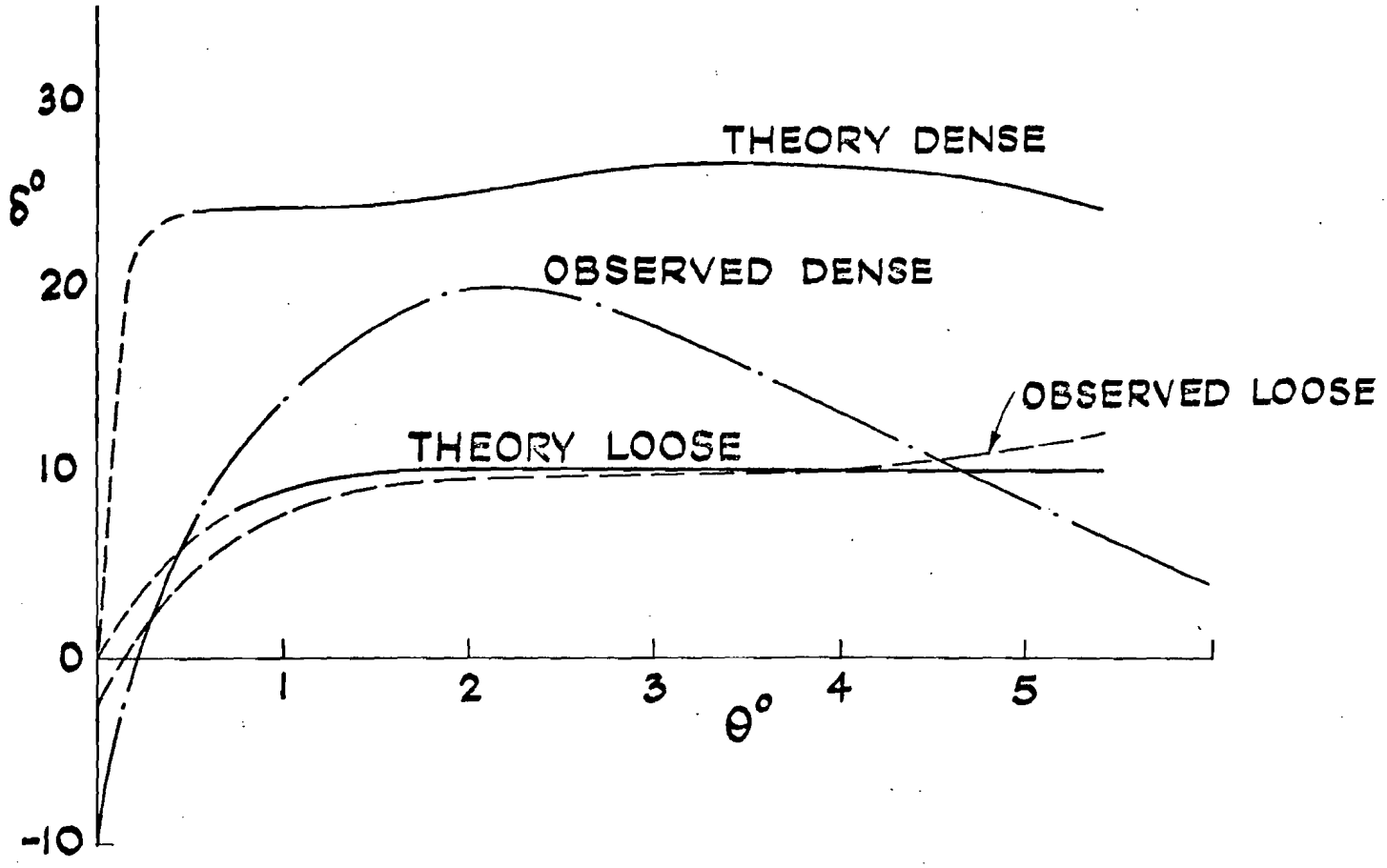

FIG. 22. MOBILIZED ANGLE OF WALL FRICTION - WALL ROTATION RELATIONSHIPS.